

# Systems biology models for cancer immunotherapy

by

Sonja Cotra

A thesis  
presented to the University of Waterloo  
in fulfillment of the  
thesis requirement for the degree of  
Master of Mathematics  
in  
Applied Mathematics

Waterloo, Ontario, Canada, 2024

© Sonja Cotra 2024

## **Author's Declaration**

This thesis consists of material all of which I authored or co-authored: see Statement of Contributions included in the thesis. This is a true copy of the thesis, including any required final revisions, as accepted by my examiners.

I understand that my thesis may be made electronically available to the public.

## Statement of Contributions

This thesis contains work written for publication; specifically, Chapter 4, pages 41-61. Details listed below including contributions from myself (as the primary author) and co-authors:

### **Sex-related differences in the immune system drive differential responses to anti-PD-1 immunotherapy**

Sonja Cotra<sup>1</sup>, Mohammad Kohandel<sup>1</sup>, Michelle Przedborski<sup>1</sup>

<sup>1</sup>Department of Applied Mathematics, University of Waterloo

Sonja Cotra contributed to the running of simulations, the analysis of the results, and the writing and editing of the manuscript. Mohammad Kohandel contributed to the project design and editing of the manuscript. Michelle Przedborski contributed to the project design and the writing and editing of the manuscript.

## Abstract

Cancer is a complex disease that continues to affect millions of people around the world every year. With ever-improving science and technology, several forms of treatment have been introduced within the past century and continue to be developed so as to provide increasing chances of survival and comfort to patients. Particularly, the 21st century has seen the blossoming of immunotherapy methods, which exploit the natural immune system's ability to kill tumor cells. Several varieties of immunotherapy exist in order to use all sorts of immune cells, targeting specific antigens expressed on tumors or blocking checkpoints which inhibit necessary immune responses. Unfortunately, there is no perfect immunotherapy that can provide a safe and effective path to remission for every patient. Traditional clinical experimentation, while providing important insight, remains a costly option in increasing our understanding of immunotherapies against cancer. Systems biology methods provide a unique and effective channel for exploring the complex dynamics involved in tumor micro-environments between cancer cells, native immune cells and administered drugs. Resulting insight may be used to inform drug development leading to safe, effective, and personalized therapeutic routines. In this thesis, we start by providing a general overview of cancer biology starting from the cell, and systems biology. We then detail equations and parameters comprising a particular systems biology model for nivolumab, an anti-PD-1 immune checkpoint inhibitor, informed by *ex vivo* data extracted from patients suffering from head and neck squamous cell carcinoma. We then present results of an examination of sex differences in regards to patient response to nivolumab monotherapy as well as combination therapy with recombinant IL12. Here, the aforementioned model was used alongside basal immune differences between the sexes from the literature to generate virtual cohorts of male and female patients receiving these treatments. Finally, we conclude with a general summary as well as potential future directions involving a similar systems biology model describing cytokine release syndrome as a side-effect of CAR-T cell therapy.

## **Acknowledgments**

I would like to thank my supervisors, Mohammad Kohandel and Michelle Przedborski, for their unparalleled patience and perseverance in guiding me through this thesis. Their knowledge and expertise have been invaluable towards the completion of this work.

I would also like to thank Siv Sivaloganathan and Mahla Poudineh for their participation as part of the defence committee, during which they asked thought provoking questions and shared interesting observations.

Finally, I thank my friends for dealing with me over the past few years, and I thank my family, who have been asking if I have finished my thesis every week since I applied for this program (yes I have).

# Table of Contents

Author's Declaration	ii
Statement of Contributions	iii
Abstract	iv
Acknowledgments	v
List of Figures	ix
List of Tables	xii
<b>1 Cancer biology</b>	<b>1</b>
1.1 Introduction . . . . .	1
1.2 Cancer cell biology . . . . .	2
1.2.1 Normal cells and their behaviour . . . . .	2
1.2.2 Cancer cell development . . . . .	4
1.3 Tumor formation . . . . .	5
1.3.1 Hallmarks of cancer . . . . .	6
1.3.2 Heterogeneity and clonal evolution . . . . .	8
1.3.3 Intrinsic and adaptive drug resistance . . . . .	9
1.4 Immunotherapy for cancer . . . . .	10

1.4.1	Emergence of immunotherapy . . . . .	10
1.4.2	Principles of immunotherapy and relevant treatments . . . . .	10
1.5	Conclusion . . . . .	12
<b>2</b>	<b>Systems biology</b>	<b>14</b>
2.1	Introduction . . . . .	14
2.2	Key concepts . . . . .	15
2.2.1	Network theory . . . . .	15
2.2.2	Dynamics and control . . . . .	16
2.2.3	Multiscale modeling . . . . .	16
2.3	Mathematical modeling . . . . .	17
2.3.1	Differential equations . . . . .	17
2.3.2	Stochastic modeling . . . . .	20
2.3.3	Agent-based modeling . . . . .	21
2.4	Data integration and analysis . . . . .	21
2.5	Applications to cancer immunotherapy . . . . .	23
2.5.1	Tumor microenvironment . . . . .	24
2.5.2	Immunotherapy mechanisms . . . . .	24
2.5.3	Personalized therapy . . . . .	24
2.6	Conclusions . . . . .	25
<b>3</b>	<b>Supplementary information for next chapter</b>	<b>26</b>
3.1	Equations . . . . .	26
3.1.1	Modeling nivolumab administration . . . . .	26
3.1.2	Modeling recombinant IL12 administration . . . . .	31
3.2	Parameters . . . . .	33

<b>4</b>	<b>Sex-related differences in the immune system drive differential responses to anti-PD-1 immunotherapy</b>	<b>41</b>
4.1	Introduction . . . . .	41
4.2	Methods . . . . .	43
4.2.1	Systems biology approach . . . . .	43
4.2.2	Generating male and female virtual patient populations . . . . .	44
4.2.3	Simulating recombinant IL12 + nivolumab combination therapy . . . . .	50
4.3	Results . . . . .	51
4.3.1	Sex-specific differences in basal immune system . . . . .	51
4.3.2	Sex-specific responses to nivolumab . . . . .	52
4.3.3	Success of simulated recombinant IL12-nivolumab combination therapy depends on patient sex . . . . .	56
4.4	Discussion . . . . .	58
<b>5</b>	<b>Conclusion</b>	<b>62</b>
5.1	Summary . . . . .	62
5.2	Future directions . . . . .	63
	<b>References</b>	<b>66</b>

# List of Figures

1.1	The process of cancer cell division. . . . .	7
1.2	PD-1:PD-L1 complex. PD-1 (green) is shown binding to PD-L1 (purple), allowing for a pathway which may be exploited by tumors. . . . .	11
2.1	pd53/HDM-2/p19/14 ARF feedback loop. Note that the arrowheads denote positive stimulation, whereas the flat bars on the end of the links denote inhibition. . . . .	16
2.2	A model of cellular information layers gathered from omics data. . . . .	23
4.1	Molecular pathway for the previously established systems biology model used in this study. It displays interactions between immune cell populations of CD4+ $T_{H0}$ , $T_{H1}$ , and $T_{H2}$ cells, CD8+ naive and cytotoxic T-cells, cytokines IL4, IL6, IL12, and IFN $\gamma$ , dendritic cells, cancer cells, and PD-1 and PD-L1. . . . .	45
4.2	Box plots demonstrating the differences between male (blue) and female (red) virtual patients for each parameter in the subset $\Omega$ . The male virtual patient population was comprised of 1000 patients with parameters generated via Latin hypercube sampling of parameters from the ranges summarized in Supplementary Table 3 [57] The female virtual patient population was comprised of 1000 patients generated via Latin hypercube sampling of parameters, with the ranges of the parameters in $\Omega$ altered to represent the ranges expected for female patients. Specifically, parameters that do not represent a fractional cell count were multiplied by a random number between 1.1-2.0, generated individually for each parameter; while the naive and cytotoxic CD8+ T-cell fractions were limited to the bottom 50% of the sampling range used for male patients. For parameters $\rho$ and $\lambda$ , the log (base 10) of the parameter values are depicted. . . . .	53

4.3	Difference in response rate for several female virtual patient populations (A-E) compared to the reference male population. All female populations were generated by multiplying the lower and upper bounds of the sampling ranges for each non-fraction sex-specific kinetic parameter in $\Omega$ by random factors in the range [1.1,2.0]. The different populations were generated by sampling the initial naive CD8+ T cell and CD8+ cytotoxic T cell populations from different ranges. Specifically, population A was generated with the CD8+ naive % and CD8+ cytotoxic % both confined to the bottom 80% of their LHS bounds. Population B features the same parameters further confined to the bottom 50% of the LHS bounds. For populations C, D, and E, only the CD8+ naive %LHS range was lowered to the bottom 50%, 10%, and 5% respectively whilst the CD8+ cytotoxic % remained unaltered as in the male population. . . . .	54
4.4	Histograms of the ratio of cancer population after treatment vs initial cancer cell count - just putting these here for now. A: male responders, B: male nonresponders, C: female responders, D: female nonresponders. Female population was generated with sex-related alteration factors in the range [1.1, 2.0] with naive and cytotoxic T-cell fractions limited to the bottom 50% of the original range. Both male and female populations comprise of approximately 1500 patients each. . . . .	55
4.5	Recombinant IL12 simulations for male (M) and female (F) patient populations with administration times up to 24h prior to nivolumab. A: RIL12 dose of 0 pg/mL. B: RIL12 dose of 10 pg/mL. Conversion rate refers to the percentage of nonresponders to nivolumab alone who converted to responders following the addition of simulated RIL12 to the treatment schedule. Male patient results are denoted by the blue line, female patient results are denoted by the red line. . . . .	57

4.6	<p>Simulated patient cancer cell counts in response to recombinant IL12 administered 24 hours prior to nivolumab. Graph A represents cancer cell count in a virtual population of 50,000 male patients and graph B represents the same for a virtual population of 50,000 female patients. In both graphs, the blue curves represent nonresponders who had successfully converted to responders with the combination treatment, while the red curves represents nonresponders who did not demonstrate improvement with the addition of RII12. Notice the increased presence of blue lines curving downward in the female population, indicating cancer cell regression. Notice also the lower average initial cancer cell populations in the female population than the male population. . . . .</p>	58
5.1	<p>Network illustrating interactions between CAR8 and CAR4 cells (blue), key inflammatory cytokines (yellow), endogenous immune cells (purple), and cancer cells (red). Pointed arrowheads indicate upregulation while flat arrowheads indicate inhibition. . . . .</p>	64

# List of Tables

3.1	Description of the kinetic parameters in the mathematical model . . . . .	33
3.2	Values and ranges of the kinetic parameters, initial protein levels, and initial T-cell populations used for virtual patient simulation and local/global sensitivity analysis . . . . .	36
4.1	Sex-specific differences in basal immune system reported in the literature and associated model parameter(s) that were modified to capture the respective sex difference . . . . .	47

# Chapter 1

## Cancer biology

### 1.1 Introduction

While Stonehenge was being constructed in England, a case of cancer was recorded for the first time about 4000 kilometers away by an unknown ancient Egyptian compiling the oldest known work on surgical trauma [1]. In what is now known as the Edwin Smith Papyrus, the writer described a bulging tumor of the breast as a grave disease with no treatment for it [2], thus setting the stage for an ongoing 5000 year-long battle against the uncontrolled proliferation and spread of abnormal cells within the human body. Despite countless new remedies across several millenia supplemented by ever-progressing scientific knowledge and understanding of this unnerving phenomenon, cancer continues its relentless assault in several forms which altogether serve as the second leading cause of death across the globe [3].

While surgical removal and treatments of tumors had already been practiced for several centuries prior, it was not until around 400 BCE that Greek physician Hippocrates proposed a scientific theory for the cause of cancer [4]. Carcinoma, as he referred to it, as well as every other disease, were then attributed to a disruption in the balance between the four body humours: blood, phlegm, yellow bile, and black bile. This hypothesis maintained dominance for hundreds of years all the way into medieval times [5], waning in popularity with the immense advancement of scientific knowledge and techniques that defined the Renaissance. With the invention of the microscope in the late 16th century, researchers had the ability to investigate tumor structure in an unprecedented capacity and therefore further the understanding of what exactly cancer is and how it operates. Specifically, Virchow proposed the notion that cancer is a disease regarding cellular lesions [6], a view

that came to be widely accepted towards the tail end of the 1800s. Now that the issue of abnormal cell division was understood, the scientific and technological advancements of the last century allowed for important discoveries regarding genetic and viral components of cancer development [4], as well as numerous breakthroughs in screening and treatment [7].

Today, we recognize cancer as an umbrella term for diseases involving the uncontrolled growth and spread of unhealthy cells in blood, tissue, bone, and several organs, with potential for invasion towards the entire body. Occurring as a result of various genetic, environmental, and viral factors, cancer remains a daunting possibility, if not a haunting reality, for people around the world. Locally, about 2 out of 5 Canadians will be diagnosed with cancer in their lifetime and 1 in 4 of them will die due to this disease [8]. With a plethora of modern methods for early detection and medical intervention, physicians and scientists continue to tackle the question of a cure. This chapter discusses the biological mechanisms behind tumor development and immunotherapy for cancer, with a particular focus on anti-PD-1 immune checkpoint inhibitors and CAR T-cell therapy.

## 1.2 Cancer cell biology

Cells are the fundamental unit of structure and function for all organisms. Since cancer is a disease characterized by mutated and uncontrolled cells, a thorough comprehension of cell biology is a key component of understanding the various mechanisms employed by tumors towards their development and vitality. Here we continue to discuss the features of healthy cells and how they pertain to the emergence and survival of cancer cells.

### 1.2.1 Normal cells and their behaviour

Multicellular organisms are comprised of eukaryotic cells, which contain a nucleus as well as other important organelles with specialized roles contributing to overall function. Highly organized and complex, eukaryotic cells are enclosed within a physical barrier and maintain a uniform basic chemical composition. In particular, cells are mainly composed of water, inorganic ions, and biomolecules, the latter of which can be divided into four major classes: nucleic acids, proteins, carbohydrates, and lipids [9]. Each of these building blocks define key operational characteristics vital to cells and by extension the beings that they form.

Nucleic acids are very large molecules consisting of several repeated units of phosphate and sugar, with a backbone of sugar groups attached to a nucleotide base. They are catego-

rized into two primary types: the double-stranded deoxyribonucleic acid (DNA) is stored in the nucleus and represents the genetic material of the cell, while the single-stranded ribonucleic acid (RNA) harnesses its ability to move around the cell to partake in various cellular activities. Specifically, messenger RNA (mRNA) is involved in delivering genetic information from DNA to the ribosomes, which in turn perform protein synthesis within the cell with the aid of ribosomal and transfer RNA. Proteins, in turn, prove vital for most cellular activities. Both DNA and RNA are comprised of four nucleotide bases adenine, cytosine, and guanine; they differ at the fourth bases of thymine and uracil respectively. With the ability to direct their own self replication, the nucleic acids serve as the fundamental informational molecules within a cell [10].

The synthesis of proteins by RNA allows for several more cellular functions to occur. Formed as a sequence of amino acids linked together by peptide bonds, proteins have a complex structure comprised of primary, secondary, tertiary, and quaternary levels. The primary level simply describes the aforementioned sequence of amino acids, of which there are 20 standard types. The secondary level involves the arrangement of these amino acids within regions of the protein, most commonly as an alpha helix or a beta pleated sheet. Tertiary structure involves the folding of the first two levels into more complicated shape as a result of interactions between the side chains of amino acids in different parts of the primary sequence; most proteins contain combinations of alpha helices and beta sheets connected by loop regions and folded into compact structures known as domains, which are the basic units of the tertiary structure. Finally, the quaternary level contains the interactions between the different polypeptide chains. Due to the wide variety of amino acids and folding methods available, proteins represent a diverse group of macromolecules responsible for several functions relating to movement, structure, regulation, signalling, transport, and catalysis; the latter of which is fundamental for nearly all chemical reactions within biological systems.

Another class of macromolecules that serves structural and nutritional functions in cells is carbohydrates, which are further classified as mono-, di-, oligo- and poly- saccharides. Generally composed of carbon atoms bonded to water molecules, carbohydrates supply the body with energy it needs to function, with simple sugars being major nutrients of cells. In animal cells, this energy is stored as glucose in glycogen, a polysaccharide dedicated to this purpose in a similar manner to starch in plant cells. Carbohydrates located on the surface of the cell may link to proteins and lipids to form glycoproteins and glycolipids, which enable further important actions. For example, glycoproteins formed by oligosaccharides serve as markers to target proteins for transport to the cell surface or in subcellular organelles. Due to their diversity, oligo- and polysaccharides in general may serve as markers on the surface to distinguish cells from one another.

Unlike the first three important biomolecules involved in cellular structure, lipids are not polymers and are classified on the basis of their insolubility in water. With functions relating to energy storage, metabolism, and drug delivery, lipids are a significant part of the cell membrane structure. Specifically, the cell membrane is a bilayer of phospholipids, each of which are two hydrophobic fatty acids (the simplest lipids) joined to a hydrophilic polar phosphate head. This allows for the properties of partial water solubility and partial water insolubility, which is the basis for the formation of biological membranes. Cell membranes also contain other lipids such as glycolipids and cholesterol, the latter of which may be derived into steroid hormones, such as estrogens and testosterone, which in turn function diversely as chemical messengers.

### 1.2.2 Cancer cell development

While there are widely accepted environmental and otherwise non-genetic factors that contribute to tumor development, cancer is a genetic disease. Driven by mutations in cancer susceptibility genes, such as oncogenes and tumor suppressor genes, cancer results from the effects of these genetic mutations on cell behaviour. Cancer susceptibility genes can be described by three main classes: gatekeepers, caretakers, and landscapers [11]. Gatekeeper genes, comprising oncogenes and tumor suppressor genes, directly regulate the growth and differentiation pathways of the cell. When these genes are mutated, the cell cycle may be disrupted and cancerous cells begin to divide uncontrollably. For instance, the retinoblastoma gene *Rb* is a tumor suppressor gene that arrests the cell cycle in instance of damaged cells; naturally, its mutation leads to the development of tumors via unregulated cell proliferation, specifically retinoblastoma [12]. Caretaker genes refer to those that maintain genomic integrity of the cell; mutations on these genes promotes tumorigenesis indirectly by destabilizing the genetic environment, leading to a rapid accumulation of changes in the oncogenes and tumor suppressor genes that control cell birth and death. Such genes include *p53*, which plays an important role in aiding the recovery of a genome from damaging mutations. Defects in *p53* will inhibit the cell's ability to care for its DNA, leading to higher rates of mutation [13]. Thirdly, landscaper gene, as the name suggests, tend to the microenvironment of the cell, with mutations leading to an abnormal environment causing neoplastic transformation of normal cells into tumor cells. While mutations of these types of genes may occur on their own quite often, the development of malignant and invasive cancer requires multiple mutations.

A key cell function disrupted by mutated genes is proliferation. Eukaryotic cells proliferate via a process called mitosis, where the nucleus and the cytoplasm of the cell are divided into two genetically identical daughter cells. In the human body, tissues are divided

into compartments containing cell populations that proliferate to fulfil organ tasks. These compartments are subject to homeostasis, whereby the division rate of the cell population matches the death rate in order to maintain stability. Thus, mutated oncogenes may increase proliferation [14] such that the proliferation rate of the cell population exceeds its death rate, thus disrupting homeostasis and potentially leading to cancer.

While the proliferation-to-death ratio may be increased directly via the effects of proliferation-inducing oncogenes, it may also be affected by a lowered cell death rate. Apoptosis refers to the mechanism by which eukaryotic cells commit suicide [15] if they are defective or otherwise unwanted within the cellular population. Mutations on oncogenes and tumor suppressor genes may affect the signalling necessary for inducing apoptosis, thus disrupting homeostasis in a given tissue compartment and leading to cancer. In particular, about half of all human cancer cases result due to mutations in *p53*, a tumor suppressor gene that causes apoptosis or cell cycle arrest in the event of damaged cell DNA. Without proper regulation of genetically faulty cells, homeostasis within the cell population is broken, paving the way for malignant tumors in the system.

When cells proliferate, it is important that their genetic material gets properly passed on to offspring in order to maintain function within their respective environment. As a result, the existence of mechanisms for addressing DNA-related issues is vital for cellular health. During the DNA replication process that occurs during mitosis, base pairing errors may occur where nucleotides are paired incorrectly, leading to deformities in the structure of the final DNA molecule [16]. This natural occurrence calls for the services of DNA polymerase, which essentially acts as a proofreader for DNA during replication: deleting the defective pair and replacing it with the correct nucleotide. Additionally, DNA molecules may be damaged on a daily basis by several factors such as UV radiation, ionizing radiation, and free radicals, which can lead to structural issues and mutation. In order to combat this, DNA repairing enzymes cut out damaged/mutated DNA while DNA polymerase and ligase use an undamaged DNA template (if available) to insert the correct nucleotides into the removed portion. Naturally, should these repair mechanisms be tampered with, mutated DNA will persist in the cell cycle leading to the development of cancer.

### 1.3 Tumor formation

There is a great deal of evidence to suggest that tumors develop in humans via a multistep process, where each step is reflective of certain genetic alterations that cause normal human cells to transform into malignant cancers. In particular, cancer cells are defective in circuits regulating cell proliferation and homeostasis. Such defects promote the development

of malignant tumors, which can be aggressive and invasive. A total of eight biological capabilities have been identified [17], [18] as those acquired during the development of tumors, known as the hallmarks of cancer.

### 1.3.1 Hallmarks of cancer

The hallmarks of cancer are listed and described below:

- **Unrestrained proliferation**

As previously established, unrestrained proliferation is a fundamental aspect of cancer cells which allows them to flourish and invade tissues in the human body. Thus, it is important for these malignancies to sustain proliferative signaling. There are multiple ways in which they may achieve this, such as through autocrine proliferative stimulation and over-expressed receptors to growth signals. They also may stimulate normal cells around them to supply growth factors.

- **Evasion of growth suppressors**

In normal cells, growth suppressors such as TGF- $\beta$  will maintain cellular quiescence by not allowing cells to pass the restriction point in the cell cycle, sending them straight to quiescence for repair. Such growth suppressors may be evaded by their inactivation, leading to a continuation of the cell cycle and thus further multiplication.

- **Resisting apoptosis**

Largely influencing the attrition of cell population, apoptosis depends upon the balance of pro- and anti-apoptosis signals. Tumor cells resist programmed cell death in a variety of ways, such as mutating to lose a pro-apoptotic regulator. Commonly, this involves the inactivation of the pro-apoptotic p53 tumor suppressor gene, as seen in more than half of human cancers. Additional resistance may involve the mitochondria-mediated intrinsic apoptosis pathway, which is regulated by members of the BCL-2 protein family. Specifically, the BCL-2 oncogene has anti-apoptotic properties and can disrupt this pathway when overexpressed. BCL-2 is upregulated in cancers such as follicular lymphoma and can contribute to the formation of B-cell lymphomas when coexpressed with the *myc* oncogene. Thus, by resisting apoptosis, tumor cells can expand in population uncontrollably.

- **Limitless replicative potential**

Normal human cells will eventually cease replication after a certain number of times. This is due to the gradual degradation of telomeres, which are protective caps on the

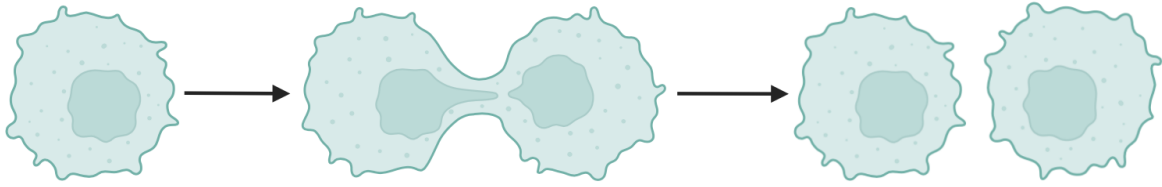


Figure 1.1: The process of cancer cell division.

ends of chromosomes, during the repetition of cell division. Eventually, the telomeres will degrade to put the cell in a state of senescence, where the cell can no longer divide. Tumor cells acquire limitless replicative potential through their possession of telomerase, an enzyme which adds telomeres to the end of a chromosome. The addition of telomeres means that the telomeres will not be able to degrade to the point of cells reaching senescence, and the cell will continue to divide indefinitely.

- **Sustained angiogenesis**

Angiogenesis is the process of forming new blood vessels from pre-existing vessels. The oxygen and nutrients supplied through blood vessels are important for cell function and survival, so all cells reside within  $100\ \mu\text{m}$  of a capillary [10]. Despite the importance of oxygen and nutrients, normal cells initially lack the ability to induce angiogenesis, restricting their capability to expand in size. Tumor cells must bypass this to expand. They induce angiogenesis through shifting the balance between pro- and anti-angiogenesis regulators in favor of angiogenesis inducers. A common way for this shifting to occur is through altered gene transcription resulting in an increased expression of angiogenesis inducers such as VEGF or FGFs, and a lowered expression of inhibitors, such as thrombospondin-1 or  $\beta$ -interferon. Although angiogenesis is thus encouraged in tumor cells, tumor vasculature is abnormal, causing the tumor microenvironment to be hypoxic, acidic, and have a high interstitial fluid pressure. All of these factors promote cell proliferation, for example hypoxia leads to the production of HIF-1 $\alpha$ , which further increases the presence of growth factors such as VEGF. Thus the angiogenesis of tumor cells helps tumor cells to expand, leading to malignant tumors.

- **Tissue invasion and metastasis**

Tumor cells acquire the ability of tissue invasion and metastasis, leading to the invasive property of malignant tumors. Metastases, the distant settlement of tumor cells to sites far from their origin, is the cause of 90% of human deaths from cancer

[19]. Successful invasion and metastasis of tumor cells depends on the previous five hallmarks discussed. One example of a mechanism supporting this function is the inactivation of E-cadherin, a homotypic cell-to-cell interaction molecule which results in the transmission of anti-growth signals. Interference with this function enhances the tumor cells capabilities to invade and undergo metastasis. The process of invasion and metastasis is a multistep process, starting with localized invasion, followed by the intravasation of cancer cells into nearby vessels. Then, these cells are transported through the circulations leading into the parenchyma of distant tissues, also known as extravasation. From here, a small tumor will form (micro-metastasis), and finally these small tumors grow into large tumors (macro-metastasis).

- **Avoiding immune destruction**

As the above described six hallmarks encourage growth and replication, tumor cells continuously evolve, and their DNA constantly mutates and adapts to their environment, allowing for them to thrive. Mutations in genes such as BRCA1, BRCA2, P53, and RB1 particularly increase the likelihood of developing cancer. Chronic inflammation causes normal cells to develop mutations and resistance to apoptosis, turning them into tumor cells. For example, tumors can evolve to express the programmed death ligand 1 (PD-L1) protein to bind to the programmed cell death 1 (PD-1) protein on immune cells, leading to the suppression of T-cell activity [20]. Cells can also recruit leukocytes, such as neutrophils and macrophages, which release cytokines and growth factors encouraging tumor growth.

- **Deregulating cellular energetics**

Tumor cells reprogram their energy metabolism by specifically reprogramming their glucose metabolism. This is done by limiting their energy metabolism mostly to glycolysis leading to aerobic glycolysis. Cancer cells compensate for the resulting lower ATP efficiency by upregulating glucose transporters such as GLUT1, increasing glucose import into the cytoplasm.

### 1.3.2 Heterogeneity and clonal evolution

Diversity plays a large role in a tumor's ability to thrive in the complex biological environments provided by human blood, organs, and tissues. Indeed, as cancer continues to grow, heterogeneity prevails as an assorted mix of cells forms the bulk of tumors [21]. Cell heterogeneity may be spatial, resulting in non-uniform distribution of tumor cell sub-populations of distinct genetic variations across and within numerous diseased locations, or temporal,

where the molecular tumor structure evolves over time. This allows for a dynamic disease that can foster immune and drug resistance.

Genetic instability is a prime enabler of heterogeneity in tumors. As discussed in previous sections, DNA can mutate due to several external factors, such as UV radiation and tobacco smoke, and internal issues regarding DNA replication and repair. With all aspects by which genetic mutations can occur, it is natural that a wide variety of different mutated cells are formed to serve as the start of a booming diversified community. Of course, genetic instability alone will not adequately support a heterogeneous abode; it is important that these mutated cells can proliferate in an adaptive manner in order to maintain malignancy. Known as clonal evolution, the generally accepted model by which clonal diversity is maintained was described first by Peter Nowell in 1976 as a Darwinian evolutionary process driven by step-wise cell mutations with consecutive trait selection [22]. Essentially, Nowell postulated that cancer cells acquire particular phenotype traits advantageous to expansion, proliferation, migration, and invasion via mutational and epigenetic alterations during division. As a result, advanced tumors will be highly complex and able to evade treatment.

### 1.3.3 Intrinsic and adaptive drug resistance

Resistance to treatment may be intrinsic or adaptive. Intrinsic resistance refers to a lack of necessary immune activity and repressed anti-tumor responses from T-cells that is present before the introduction of therapy to the system [23]. This phenomenon is observed among immunocompromised patients, such as those living with HIV or transplanted organs, as well as elderly patients; these patients may be unable to elicit appropriately potent immune responses to several foreign antigens. Intrinsic resistance may also arise independently from the quality of innate immune functions, instead resulting from particular tumor phenotypes. As discussed above in Section 1.3.2, cancer cells acquire traits that serve their survival. Some tumors may express very few antigens that are viewed as foreign to the immune system, instead overexpressing antigens that are also present in healthy tissue. This allows for effective immune evasion. Due to intrinsic resistance, both immunotherapies and targeted therapies may prove ineffective for certain patient populations.

Adaptive resistance may be either natural or drug-induced. Unique to immunotherapy, naturally acquired resistance is not necessarily induced by it but instead results from naturally occurring immune pressure upon a tumor. Drug induced resistance occurs in cases where patients may respond initially to treatment but experience relapse after a period time. Both of these adaptive resistance types share general mechanisms depending

on a local equilibrium between effector T-cells and tumor cells. Eventually, due to complex feedback mechanisms including the expression of checkpoint molecules [24] that inhibit T-cell function as well as clonal evolution, tumors eventually gain dominance over T-cells, rendering treatments and immune intervention ineffective [23].

## 1.4 Immunotherapy for cancer

With millions of deaths resulting from cancer each year across the globe, scientists and physicians must work together to develop treatments to prevent, absolve, or at least delay the growth of malignant tumors. Therapeutic intervention takes a multitude of forms, such as surgery, chemotherapy, and radiotherapy, all of which have been in use for decades [25]. Since tumors attack various different parts of the body and exhibit staggering genetic diversity, which is in turn multiplied by the natural physiological diversity in the millions of patients in whom they reside, it is important that cancer treatment itself can also present diversely in order to treat all kinds of patient and cancer presentations. Indeed, no existing treatment provides a universal cure for all patients, with many requiring targeted and personalized treatment plans and perhaps even combination therapies.

### 1.4.1 Emergence of immunotherapy

Among the many strategies devised to treat cancer, immunotherapy has provided much promise in recent years. While the concept of therapeutic interference for enhanced immune response to disease goes back to ancient times [26], oncological applications began in the late 19th century and picked up speed only in the 1960s. Building upon centuries of study regarding immune cells and their functions, several immunotherapies are FDA approved as first-line therapies [26] to combat the many cancer types with a large variety of immune cells. These include the primary categories of cancer vaccines, cytokine therapies, adoptive cell transfer, immune checkpoint inhibitors, and oncolytic virus therapies [27]. This thesis in particular focuses on anti-PD-1 immune checkpoint inhibitors and the adoptive cell transfer CAR T-cell therapy, so they are discussed in more detail in the following section.

### 1.4.2 Principles of immunotherapy and relevant treatments

Immune effector cells such as lymphocytes, macrophages, natural killer cells, and others work to target abnormal antigens, thus providing a defense against tumor cells in the human

body; however, as discussed previously, well-developed tumors will use clonal evolution and genetic diversity to evade attacks from these cells. Thus, several different immunotherapy treatments have been developed to harness the anti-tumor abilities of these cells in an explicit and targeted effort to eradicate malignant cells as much as possible.

A particular type of immunotherapy which pertains to later chapters of this work is known as immune checkpoint inhibitors, abbreviated as ICIs. Immune checkpoints are molecules that act to regulate immune tolerance via co-inhibitory signalling pathways. Unfortunately, cancer cells will exploit these molecules, such as programmed cell death 1 (PD-1) and cytotoxic T lymphocyte antigen (CTLA-4), via their negative regulation of T-cell-mediated immune responses, thus effectively evading immune surveillance [27]. Specifically, PD-1 is expressed on the surface of several immune cells such as T-cells, NK-cells, and monocytes within the tumor microenvironment and, when bound to its ligand PD-L1 (as seen in Figure 1.2), leads to the suppression of lymphocyte proliferation and the secretion of cytokines such as IL-2, IFN- $\gamma$ , and TNF- $\alpha$  [20]. Tumor cells thus escape the immune system by exploiting the PD-1/PD-L1 pathway with expression of abnormally high levels of PD-L1. In order to combat this, anti-PD-1 ICIs selectively target and block the interaction between PD-1 and PD-L1 in order to ensure an increase in anti-tumor activity by immune cells.

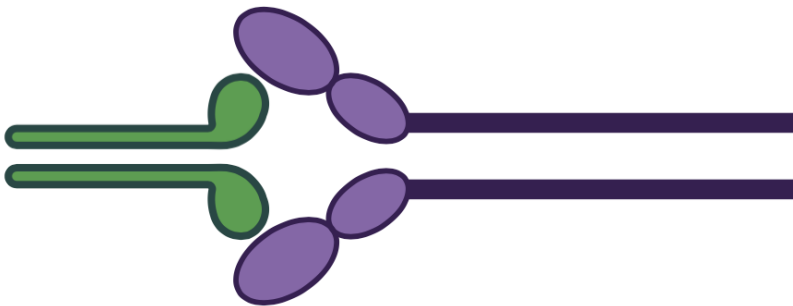


Figure 1.2: PD-1:PD-L1 complex. PD-1 (green) is shown binding to PD-L1 (purple), allowing for a pathway which may be exploited by tumors.

Another form of immunotherapy that has grown considerably as of late is CAR T-cell therapy. CAR T-cells refer to T-cells which have been genetically engineered to express chimeric antigen receptors (CARs). Allowing antibody redirected and major histocom-

patibility complex (MHC)-independent target cell killings, this modification to T-cells is crucial in overcoming of three main hurdles [28] posed by tumors. Firstly, the reduction of the expression of MHC class I and costimulatory molecules diminishes the unmodified T cell's antigen recognition capabilities, as well as its delivery of strong intracellular signaling cascade required for productive anti-tumor cytotoxic responses. The lack of costimulatory molecules in the tumor microenvironment further leads to anergy in the unmodified T cell, thus eliminating its ability to produce cytokines and compromising its proliferation and tumor-killing activities. Lastly, the unmodified T cell tends to tolerate tumor cells. When formed in the body, T-cell receptors learn to recognize non-self antigens and ignore self-antigens, so as not to attack healthy host tissue. Unfortunately, most tumors express self-antigens, escaping immunosurveillance. CARs allow the T-cell to recognize specific self-antigens expressed by tumor cells, effectively targeting the cancer.

## 1.5 Conclusion

Notorious as it is on a global scale, cancer proves to be a devastating disease through the sustained alterations on normal cell biology. With the help of several defined hallmarks, tumors emerge and progress to dominate organs, spread across the entire body, and resist as many attempts at treatment as they can. As a result, it is important to continue to understand the complexities of cancer biology in order to develop safe and effective therapeutic options for a diverse array of patient profiles. While several therapies have existed for several centuries, immunotherapy shows promise in recent years, entailing the pharmaceutical harnessing of innate immune cell functions which may be hindered by tumor cells. Indeed, various types of immunotherapy, such as ICIs, CAR T-cell therapy, and many more, prove successful for particular cancer cases with their unique function allowing for patient-specific treatment regimens.

The following chapter details system biology, the usage of mathematical and computational tools to model and analyze biological systems. Systems biology can serve as a powerful tool for understanding the dynamics that occur within tumor microenvironments, taking into account the effects of tumor cells, endogenous immune cells and tissue, as well as any sort of pharmaceutical intervention that may be applied. Given the complexity and volume of variables within the human immune system, systems biology provides a safe and cost-effective alternative to clinical trials as a means for the necessary development and optimization of targeted or combination therapies. This will inevitably provide valuable insight regarding personalized therapy, thus improving treatment outcomes for patients with all sorts of cancer types and individual immune characteristics. Subsequent chapters

discuss methodology and results of a particular project utilizing a previously established systems biology network and virtual patient simulations to examine differences between male and female patients in their response to nivolumab, an anti-PD-1 ICI. Finally, the thesis concludes with a summary as well as a discussion of future directions regarding the applications of systems biology to immunotherapy in cancer. Specifically, we will introduce as a potential future work a mathematical model of cytokine release syndrome resulting from CAR T-cell therapy and more future directions regarding the applications of systems biology to immunotherapy in cancer.

# Chapter 2

## Systems biology

### 2.1 Introduction

The human body is made up of many distinct systems that thrive off interactions between and within one another, allowing for proper function and survival. Systems biology refers to the study of the complex interactions and characteristics of components within these systems and has gained traction in biological research since the beginning of the 21st century [29]. Often defined as an interdisciplinary process, systems biology research often employs mathematical and computational tools [30] to understand biological networks in unexplored ways, leading to new discoveries and increased understanding regarding cellular and molecular behaviour in a variety of contexts.

While several disciplines such as astronomy and economics have utilized systems theory for hundreds of years [31], it was not until the 20th century that it was applied to biological research. Instead, early biological investigation opted for a mechanistic reductionist approach stemming from the Cartesian idea that complicated circumstances can be reduced to more manageable pieces, the analysis of which may be used to reassemble the whole system via the behaviour of each individual piece [29]. Indeed, early 1900s scientists understood biological organisms as complex machines with predetermined behaviours uniform across an entire species. Naturally, the mechanistic reductionist view had limitations which ultimately led to scientific objection and a turn towards systems biology methods as a preferred lens via which to study the natural and human sciences. During the early-to-mid 1900s, then, several strides have been made to understand biological systems as a hierarchy of organisation informed by communication and control networks.

As of now, systems theory has contributed to fascinating progress within several areas of biology such as molecular biology, ecology, genetics, and many more. This chapter will provide a general overview of the concepts vital to systems biology as well as integration of mathematics and data in systems-based methodology. Afterwards, applications to cancer immunotherapy will be discussed so as to provide satisfactory background information for subsequent chapters detailing specific implementation of systems biology to better understand immunotherapy mechanisms in cancer patients.

## 2.2 Key concepts

Systems biology relies on several integral ideas in order to properly serve as a vehicle of understanding for biological structures and their behaviours. A general overview of the concepts of network theory, dynamics and control, and multiscale modeling will be discussed below so as to supply ample context pertaining to systems biology methodology.

### 2.2.1 Network theory

Biological systems are studied through the lens of networks in which molecular components such as cells and proteins are treated as nodes that are linked together directly or indirectly via their interactions [32]. As such, systems biology utilizes network theory, which provides a mathematical framework via graph theory. Specifically, a network is a type of graph in which nodes and links possess individual attributes contributing to the overall behaviour and function of the system. Various types of graphs, and thus networks, can exist; in this study, the directed network is of particular interest. A directed network refers to a network where the links, representing cellular interactions, are represented by arrows in order to provide directional and type of interaction. Biological systems benefit from a semantic approach [33] in which different types of arrows are used to indicate directed relationships such as inhibition, enhancement, and cell killing, all present within a tumor microenvironment for example. Such semantic links are exemplified in Figure 2.1 These links may connect nodes to other nodes, or even to other links, indicating in this case that the presence of a particular node may have consequences on a particular interaction between two other nodes. Networks may be used to represent signalling or regulation, both key functions within a biological system.

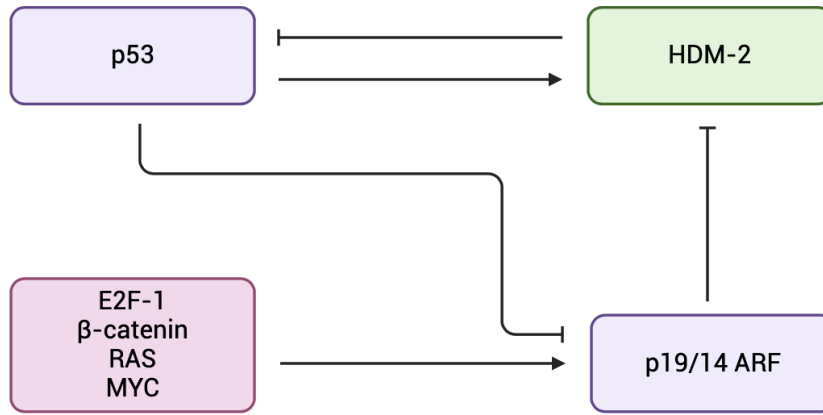


Figure 2.1: p53/HDM-2/p19/14 ARF feedback loop. Note that the arrowheads denote positive stimulation, whereas the flat bars on the end of the links denote inhibition.

### 2.2.2 Dynamics and control

Another tenet of systems biology is control theory, an engineering and mathematical discipline that allows for analysis of complex cellular and molecular dynamics via the principles of regulation and feedback control [34]. Several biological networks involve feedback loops in which the output of a particular system may affect that same system via amplification (positive) or inhibition (negative). For example, the p53 regulation of the cell cycle and apoptosis involves multiple feedback loops [35], one of which is illustrated in Figure 2.1 above. Here, oncogenes such as E2F-1,  $\beta$ -catenin, MYC, and RAS activate p53 via a positive feedback loop leading to increased p19 or p14 ARF, which in turn inhibits HDM-2 ubiquitin ligase. Since HDM-2 inactivates p53, its inhibition via the feedback loop represents an indirect promotion of p53 activation [36].

### 2.2.3 Multiscale modeling

Due to the inherent complexity of biological systems, multiscale modeling is required to properly encapsulate their functions and behaviours. Such modeling takes into account the array of temporal and spatial domains over which these systems operate, such as basic amino acid substitutions and coordinated signalling cascades regulating hormone release over the entire life of an organism [37]. From the amino acids that make up proteins

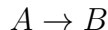
that in turn contribute to cell structure and function, all the way to tissues and organs, multiscale modeling can examine the hierarchical structures that comprise the human body [38]. Indeed, while biological systems are not simply the sum of their parts, it is important to take note of each level within biological organization as well as the interactions between these levels that contribute to the organism as a whole.

## 2.3 Mathematical modeling

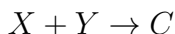
Mathematical interpretations of biological systems has proven invaluable to furthering the understanding of dynamics and interactions within networks. With a vast array of methods and application, mathematical models aid in the prediction of how biological systems may behave under an endless array of conditions, thus cementing themselves as practical tools in clinical and scientific work.

### 2.3.1 Differential equations

Employed in a wide range of contexts and fields, ordinary differential equations are powerful devices for representing rate of change over time for all kinds of different variables. In systems biology, biological interactions such as upregulation and inhibition are translated into rate equations, allowing for modeling of each of the system's components and thus the system as a whole. These differential equations are commonly constructed using the law of mass action, which states: the rate of a chemical reaction is proportional to the product of the concentrations of the reactants [39]. Thus, for the following reaction



the rate of the reaction would be  $\alpha_1[A]$  where  $[A]$  is the concentration of  $A$ . Similarly, for the reaction with two reactants rather than one:



the rate of the reaction would be  $\alpha_2[X][Y]$ . Naturally, the same logic applies for cases with more reactants. In the case of repeated identical reactants, take the example



Here, the rate of reaction would be  $\alpha_3[Z]^2$ . The exponent on each reactant in the rate law is known as the kinetic order of the reactant within the reaction; here,  $Z$  has kinetic order

2 whereas in the above equations,  $A$ ,  $X$ , and  $Y$  all have order 1. A reaction that occurs without an explicit reactant would be a zero-order reaction, where the rate of the reaction is constant.

In the above reactions,  $\alpha_1$ ,  $\alpha_2$  and  $\alpha_3$  are proportionality constants. These constants, known as rate constants, have dimensions dependent upon the number of reactants that allow for the rate of reaction itself to be represented in concentration  $\cdot$  time<sup>-1</sup>. Thus,  $\alpha_1$  has units time<sup>-1</sup>, whereas  $\alpha_2$  and  $\alpha_3$  have units concentration<sup>-1</sup>  $\cdot$  time<sup>-1</sup>. For reactions taking place in inconsistent environments, this rate constant would be replaced by an effective rate constant, which further depends on any relevant factors that would affect the reaction rate, such as the concentrations of enzymes for example. Overall, the law of mass action is based on the idea that the probability that a reaction occurs is proportional to the probability of the reactants interacting with one another.

Applying this reasoning, differential equations modeling biological systems may take on a variety of different forms depending on the particular process or interaction they are meant to represent. For the purposes of this thesis, we will describe the mathematical representations of some common cellular functions. In particular, we will centre our discussion around a cell population  $a$  and, in incremental fashion, devise an equation with terms for each important cell process. Some notes will be made regarding modeling cytokine concentrations as they pertain to later chapters.

## Proliferation and upregulation

An important part of cell biology is proliferation, the mechanism by which cells independently sustain their population. To represent proliferation mathematically, a simple differential equation suffices. Let  $a(t)$  be the population of cell  $a$  at time  $t$ . We have

$$\frac{d}{dt}a(t) = \alpha_a a(t) \tag{2.1}$$

Here,  $\alpha_a > 0$  represents the rate at which  $a$  proliferates and has units  $time^{-1}$ . Note that cytokines are soluble molecules that do not proliferate and thus rely solely on secretion from cells. Let  $i(t)$  represent the concentration of a cytokine  $i$  at time  $t$ , and suppose it is secreted by  $a$ , then we have

$$\frac{d}{dt}i(t) = \alpha_{a-i} a(t) \tag{2.2}$$

where  $\alpha_{a-i} > 0$  is the rate at which  $a$  cells produce the  $i$  cytokine and has the units  $concentration \cdot cells^{-1} \cdot time^{-1}$ .

The complex nature of biological systems allow for several other entities, such as other cells and cytokines, to contribute to the growth of any given cell population. These contributions may not be represented by such simple terms and may employ the Hill function, for example, to properly capture the dynamics of the upregulation process. Let  $b(t)$  be the population of  $b$  at time  $t$  where  $b$  is a cell within the same system as  $a$  that upregulates the proliferation of  $a$ . Then, we have

$$\frac{d}{dt}a(t) = \alpha_a a(t) + \alpha_{b-a} a(t) \frac{b(t)^n}{q_b + b(t)^n} \quad (2.3)$$

Here, we added the second term to equation 2.1 in order to represent the above-described upregulation by  $b$  on the proliferation of  $a$ . The term  $\alpha_{b-a} > 0$  the  $b$ -dependent growth rate of  $a$  with units  $time^{-1}$ . Another new parameter,  $q_b > 0$ , would be the half-maximal  $b$  cell population for  $b$ -dependent proliferation of  $a$ , and often has the unit *cells*. Finally,  $n$  is an empirical parameter that controls the shape and steepness of the function and is typically fit to data. The simplest case is  $n = 1$ . Upregulation by a cytokine would look quite similar with parameter units altered appropriately, usually with *concentration* in place of *cells*. An example of upregulation by cytokines include IL12-facilitated proliferation of cytotoxic T-cells [40]. As for cells,  $Th_1$ -activated dendritic cells upregulate the differentiation of naive CD8+ T-cells into cytotoxic T-cells [41], [42].

### Decay and inhibition

In order to preserve a state of homeostasis, a cell population must experience natural death; of course, as discussed in the previous chapter, uncontrolled cell proliferation is a rather undesirable phenomenon. Cell death can be represented simply via a similar term as that of proliferation. Adding this term to equation 2.3, we have

$$\frac{d}{dt}a(t) = \alpha_a a(t) + \alpha_{b-a} a(t) \frac{b(t)}{q_b + b(t)} - \delta_a a(t) \quad (2.4)$$

where  $\delta_a > 0$  is the rate at which  $a$  cells die with units  $time^{-1}$ . This decay rate is related to the half-life of the cell

$$\delta_a = \frac{\ln 2}{\text{half-life}}$$

Cytokines also have a natural decay rate that behaves identically.

In addition to upregulation, cell interaction may cause the inhibition of certain cell processes. To illustrate this, let  $c$  be a cell population in the same system as  $a$  and  $b$  and let  $c(t)$  be the population of  $c$  at time  $t$ . Suppose that  $c$  inhibits the proliferation of  $a$ .

This can be added to equation 2.4 accordingly:

$$\frac{d}{dt}a(t) = \left( \alpha_a a(t) + \alpha_{b-a} a(t) \frac{b(t)}{q_b + b(t)} \right) \left( \frac{r_c}{r_c + c(t)} \right) - \delta_a a(t) \quad (2.5)$$

Since the equation for the rate of change of  $a$ 's population is impacted by two terms for proliferation, both of these terms are subjected to the inhibitory effects of  $c$ . The parameter  $r_c$  is the half-maximal  $c$  population for  $c$ -dependent inhibition of the proliferation of  $a$  and has the unit *cells*. If  $c$  were a cytokine rather than a cell, then the appropriate unit would be *concentration*.

## Differentiation

Many cell types undergo differentiation as an important part of their life cycle. Differentiation describes the transformation from one cell type into another more specialized type, often fit with particular functional abilities that serve the system in which it resides. Suppose that  $d_1$  is a cell that differentiates into  $d_2$ . Let  $\alpha_{d1} > 0$  and  $\delta_{d1} > 0$  be the proliferation and death rates for  $d_1$  and let  $\alpha_{d2} > 0$  and  $\delta_{d2} > 0$  be the proliferation and death rates for  $d_2$ . Then, let  $d_1$  differentiate into  $d_2$  at a rate constant of  $\beta > 0$  with the unit  $time^{-1}$ . Then, letting  $d_1(t)$  and  $d_2(t)$  be the respective populations of  $d_1$  and  $d_2$  at time  $t$ , we have

$$\frac{d}{dt}d_1(t) = \alpha_{d1}d_1(t) - \beta d_1(t) - \delta_{d1}d_1(t) \quad (2.6)$$

and

$$\frac{d}{dt}d_2(t) = \alpha_{d2}d_2(t) + \beta d_1(t) - \delta_{d2}d_2(t) \quad (2.7)$$

As demonstrated in equations 2.6 and 2.7 above, the same differentiation term is applied to both populations in opposite directions, as all differentiating  $d_1$  cells will decrease the  $d_1$  population and become  $d_2$  cells, increasing the  $d_2$  population by the same amount. Like any other process, differentiation may be upregulated or inhibited by other cells or cytokines.

A differential-equations based model may include several cellular and molecular populations with equations corresponding to interactions within a network. When paired with initial conditions and numerical parameters, the model can be solved as a system of equations, thus providing simulations of cell populations over a period of time.

### 2.3.2 Stochastic modeling

For smaller biological populations, the deterministic differential equation models fail to account for random fluctuations that naturally occur in the behaviours of cells and molecules

[39]. As a result, stochastic modeling may be preferred to describe processes with random elements in their dynamic progression. Discrete in nature, stochastic methods on their own often do not track individual components over time, instead focusing on the entire population [43]. That being said, individual agents may be accounted for in agent-based modeling combined with a stochastic approach. Spatial homogeneity is also assumed.

### 2.3.3 Agent-based modeling

Agent-based modeling focuses on multiple agents with autonomy within a system of pre-defined rules, which may be discrete, continuous, or both [44]. As a result, they serve as a diverse tool to describe cellular populations, with potential for the implementation of graphs, neural networks, ordinary differential equations, and/or logical statements. These models directly target the agents via a bottom-up approach and provide a framework for complex biological systems via their smaller individual components.

## 2.4 Data integration and analysis

In order for mathematical models and other systems biology methods to have any practical bearing in biological and medical research, accurate experimental data must be effectively integrated into any such study. Indeed, empirical data provides a numerical foundation for systems biology results to be meaningful and realistic within its particular context. This section will discuss the various types of data used in systems biology as well as the methods by which they are implemented.

Omics technologies refer to those that target data regarding domains in biology ending in “omics”: genomics, proteomics, metabolics, transcriptomics, and many more [45]. Including data ranging from gene expression profiling, to global protein analysis, to metabolite collection and beyond, these techniques provide quantitative insights into the dynamics and interactions present within biological environments, rendering them instrumental to systems biology methodology. Often characterized by high-throughput procedures, omics technologies offer large amounts of high-quality data boasting several advantages to traditional technologies, including ease of use, efficiency, and quick results. However, limitations do exist across the wide range of omics technologies, which may be alleviated via the usage of multiple types of these technologies to gather data from multiple sources [46]. Ultimately, omics technologies combined with systems biology supply a holistic approach to biological studies, solidifying a comprehensive appreciation of the mechanisms and functions under review.

Understanding omics is vital for data integration, which refers to the analysis of all omics layers in a biological system. Specifically, multiple data sets from various omics technologies are gathered and collectively examined in order to build a joint model capturing all datasets simultaneously [47]. These models use networks, as described in Section 2.2.1, to represent each omics level. Such organization is illustrated in Figure 2.2. Biological networks comprise of three main classes: molecular interaction networks, which focus on physical bonds among proteins and drugs, as well as reaction catalysis among enzymes; functional association networks include genetic interactions and associations between genes and diseases; and finally, functional and structural similarity networks regard hierarchical relations and similarities in expression, structure, protein sequence, and side effects of genes, proteins, and drugs. Models can further be divided based on the type of data they integrate: homogeneous integration methods consist of one type of node (for example, just proteins) linked in a variety of ways between several networks. Heterogeneous integration, which, in line with many biological data, consists of several types of nodes linked by a wide variety of interactions.

Several methods exist in order to integrate either homogeneous or heterogeneous data. Early data integration refers to the combination of multiple datasets into one onto which the model is built. Late data integration builds models for each data set which are then amalgamated into one model for the entire system. Lastly, intermediate data integration provides a increased accuracy of model prediction by combining data from the results of a joint model [47]. Despite risking information loss and reduced performance, the first two methods may be superior in certain circumstances [48].

Systems biology often employs statistical methods to analyze biological data resulting in meaningful contributions to the overall scientific understanding of relevant systems. For instance, clustering methods are often beneficial for the identifications of genes and interactions that are responsible for particular biological phenomena [49]. Hierarchical and  $k$ -means clustering are the most popular clustering methods due to computational simplicity, although they are vulnerable to artificial separation. Dimension reduction techniques such as principal component analysis may also be used to form pattern-based clusters. There are also several tools available for the analysis of pathways and networks, allowing for the grouping of biomarkers into pathways and reducing the complexity of the system. These tools rely on enrichment analyses and pathway summary statistics to identify active pathways along with important insights into their mechanisms. Enrichment analysis often involves the identification of statistically significant differences in gene expression between different conditions regarding, for example, health or treatment status, aiming to uncover dynamics such as those related to drug response [50]. This is aided by gene ontology analysis, which makes use of a knowledgebase dedicated to unifying all gene and gene product

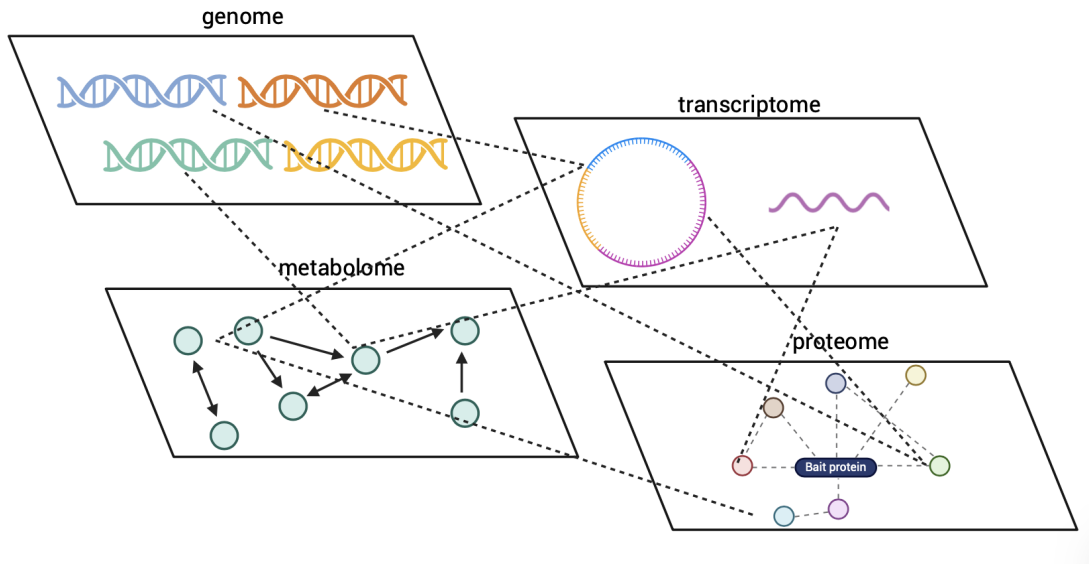


Figure 2.2: A model of cellular information layers gathered from omics data.

attributes [51]. Statistical analysis of the high-throughput data used in these networks via network inference techniques allows for the structure of the network itself to be examined. This process is unfortunately not straightforward and relies on the acquisition of several temporal data, which is frequently not collected for such experiments.

## 2.5 Applications to cancer immunotherapy

Among the everlasting efforts to develop and improve cancer treatments, systems biology provides valuable insight to help inform clinical decisions. The complexities of the immune system and its interactions with tumor microenvironments have been well represented through mathematical and computational means; the additional modelling of drug dynamics allows for efficient examination of therapeutic effects in particular patients and in-silico experimentation with differing treatment dosage plans. These applications of systems biology allow for future improvements in personalized therapy and safety for patients receiving immunotherapy.

### **2.5.1 Tumor microenvironment**

The tumor microenvironment comprises several interactions and feedback loops involving cytokines, hormones, enzymes, growth factors, and other molecules secreted and upregulated by tumor cells [52]. Systems biology approaches effectively allow for proper analysis of the heterogeneity and dynamic inconsistency within the microenvironment which may be otherwise difficult to capture precisely with laboratory techniques. The more is understood regarding the tumor microenvironment, the further the effects of treatment can be studied in order to create optimal therapeutic options.

### **2.5.2 Immunotherapy mechanisms**

Since immunotherapy exploits the functions of immune cells to combat tumors, several complex interactions take place during its administration. Systems biology methods have been used for decades now to aid in drug discovery and development by studying these interactions [53]. For instance, omics platforms and data integration have been fruitful in efforts to isolate and characterize tumor antigens which may serve as targets for any potential immunotherapies. Examples include CD19, a tissue-specific antigen on B-cells, which is targeted by some CAR T-cell therapies. These procedures have also aided in increasing understanding of the molecular pathways associated with immune surveillance of tumors, providing insight into the mechanisms which may be employed by a drug in order to effectively eliminate its target.

### **2.5.3 Personalized therapy**

An unfortunate obstacle to the development of safe, functional treatments is the innate diversity among human immune systems. That is, what could cure one patient may just kill another. In addition to providing general knowledge of tumor-immune interactions to develop immunotherapies, systems biology methods have also lent a hand to the study of precision medicine, which provides treatment plans based on individual patient factors [54]. Using omics technologies, tumor gene-expression profiling has aided in the discovery of particular biomarkers which can serve as predictive tools regarding a patient's response to a certain drug, thus informing an appropriate patient-specific treatment plan. Other diagnostic markers such as peripheral whole blood or PBMC profiles may serve the same purpose. This predictive knowledge can be incorporated into mathematical models in order to run in-silico simulations of treatment regimens, providing a cost-effective alternative

to clinical trials without risking the health of clinical trial subjects. Ultimately, systems biology has promising potential to contribute to the development of personalized therapeutic interventions fit to each individual's immune system, improving overall survival for all patients.

## 2.6 Conclusions

The study of biology has experienced much reform over the past few centuries. The integration of mathematical, engineering, and computational approaches has helped broaden the understanding of biological mechanisms with endless applications in health and medicine. Built upon network theory and dynamics, systems biology has provided important tools combined with high-throughput data to further the study of what goes on in biological organisms. With notable involvement in the advancement of cancer immunotherapy, systems biology method and omics techniques have yielded much understanding of the immune interactions within the tumor microenvironment, thus assisting the development of immunotherapies and especially personalized treatment plans. For example, a three-compartment systems biology model of CAR T-cell immunotherapy was able to simulate various dosage amounts and schedules, thus allowing for insight into how this drug may be administered so as to most effectively treat cancer [55].

Subsequent chapters will focus on a particular project employing a systems biology model to elucidate sex differences in response to the immune checkpoint inhibitor nivolumab. Methods and results will be discussed along with the structure of the model. Following this, the thesis will be concluded with a final discussion and an overview of future directions regarding systems biology methods within the context of cancer immunotherapy.

# Chapter 3

## Supplementary information for next chapter

The next chapter of this thesis discusses a project using a systems biology model from prior work [56], [57] to gauge sex differences in regards to the administration of nivolumab, an immune checkpoint inhibitor (ICI), as well as recombinant IL12 combination therapy. Before going into the details regarding the methodology and results of this project, we will first provide in-depth information regarding the equations and parameters that inform this model. The network as a whole will be discussed in the following chapter.

### 3.1 Equations

#### 3.1.1 Modeling nivolumab administration

In order to capture the dynamics of nivolumab treatment within a patient's immune system, several equations were created with the aim of capturing tumoral response in an ex vivo experimental setup. With a system of 15 coupled ordinary differential equations mathematically describing nivolumab administration and another 5 pertaining specifically to recombinant IL12 dynamics, a system is built comprising of immunotherapy drugs, cancer cells, and immune cells. Immune cell proliferation in these equations is assumed to represent mitosis, with both proliferation and death rates proportional to the population of the respective cellular species.

1. Time evolution of naive helper (CD4+) T-cell population:

$$\begin{aligned} \frac{dT_{N4}}{dt} = & n_4 T_{N4} - \left( d_{1-12} T_{N4} \frac{[IL-12]}{q_{dIL12} + [IL-12]} \right. \\ & \left. + d_{1-IFN} T_{N4} \frac{[IFN\gamma]}{q_{IFN-1} + [IFN\gamma]} \right) \left( \frac{s_1}{s_1 + [PD-1 : PD-L1]} \right) \\ & - \left( d_2 T_{N4} \frac{[IL-4]}{q_{dIL4} + [IL-4]} \right) \left( \frac{s_2}{s_2 + [PD-1 : PD-L1]} \right) \end{aligned} \quad (3.1)$$

Net proliferation of  $T_{N4}$  cells is illustrated by the first term, in line with the discussion of differential equation representations of cellular processes in the preceding chapter. The second term describes the differentiation of  $T_{N4}$  cells into  $Th_1$  cells in the presence of IL-12 [58], while the third term described the same process in the presence of IFN $\gamma$  [59]. These differentiation processes are inhibited by the PD-1:PD-L1 complex [60]–[62], as indicated by the multiplicative factor applied to terms 2 and 3. The fourth and final term describes the differentiation of  $T_{N4}$  cells into  $Th_2$  cells in the presence of IL-4 [58], [59], which is also inhibited by the PD-1:PD-L1 complex [60]–[62].

2. Time evolution of type 1 helper T-cell population:

$$\begin{aligned} \frac{dTh_1}{dt} = & n_1 Th_1 + \left( d_{1-12} T_{N4} \frac{[IL-12]}{q_{dIL12} + [IL-12]} + \right. \\ & \left. d_{1-IFN} T_{N4} \frac{[IFN\gamma]}{q_{IFN-1} + [IFN\gamma]} \right) \left( \frac{s_1}{s_1 + [PD-1 : PD-L1]} \right) \end{aligned} \quad (3.2)$$

The first term describes the net proliferation of  $Th_1$  cells. The remaining terms, similarly to terms 2 and 3 in Equation (3.1) describe the increase in the  $Th_1$  cell population due to the differentiation of  $T_{N4}$  cells into  $Th_1$  cells in the presence of IL-12 [58] (term 2) and IFN $\gamma$  [59] (term 3), which is inhibited by the PD-1:PD-L1 complex [60]–[62].

3. Time evolution of type 2 helper T-cell population:

$$\begin{aligned} \frac{dTh_2}{dt} = & \left( g_2 Th_2 + g_{2-4} Th_2 \frac{[IL-4]}{q_{gIL4} + [IL-4]} \right) \left( \frac{r_{IFN}}{r_{IFN} + [IFN\gamma]} \right) \\ & + \left( d_2 T_{N4} \frac{[IL-4]}{q_{dIL4} + [IL-4]} \right) \left( \frac{s_2}{s_2 + [PD-1 : PD-L1]} \right) - \delta_2 Th_2 \end{aligned} \quad (3.3)$$

The first term describes the proliferation of  $Th_2$  cells, with the second term denoting upregulation by IL-4 [58], [59]. This proliferation is also inhibited by IFN $\gamma$  [63] as

seen by the inhibition factor that is applied to the first two terms. The third term describes the increase in  $Th_2$  population resulting from the differentiation of  $T_{N4}$  cells into  $Th_2$  cells in the presence of IL-4 [58], [59], which is inhibited by the PD-1:PD-L1 [60]–[62] complex. The final term describes naturally occurring death of the  $Th_2$  cells.

4. Time evolution of naive cytotoxic (CD8+) T-cell population:

$$\frac{dT_{N8}}{dt} = n_8 T_{N8} - d_c T_{N8} \left( \frac{Th_1}{q_1 + Th_1} \right) \left( \frac{s_c}{s_c + [PD - 1 : PD - L1]} \right) \quad (3.4)$$

The first term describes the net proliferation of  $T_{N8}$  cells. The second term describes the process of  $T_{N8}$  cells differentiating into  $T_c$  cells, as motivated by the company of  $Th_1$  cells [41], [42]. This is also inhibited by the PD-1:PD-L1 complex [60]–[62].

5. Time evolution of cytotoxic (CD8+) T-cell population:

$$\frac{dT_c}{dt} = n_c T_c + g_{c-12} T_c \frac{[IL - 12]}{q_{gIL12} + [IL - 12]} + d_c T_{N8} \left( \frac{Th_1}{q_1 + Th_1} \right) \left( \frac{s_c}{s_c + [PD - 1 : PD - L1]} \right) \quad (3.5)$$

The first term describes the net proliferation of  $T_c$  cells. This process is upregulated by IL-12 [40], as demonstrated by the second term. The third term describes the increase in the  $T_c$  cell population that occurs when the  $T_{N8}$  cells differentiate into  $T_c$  cells, which in turn happens in the presence of  $Th_1$ -activated dendritic cells (DCs) [41], [42]. Finally, this differentiation process is inhibited by the PD-1:PD-L1 complex [60]–[62].

6. Time evolution of cancer cell population:

$$\frac{dC}{dt} = n_{Can} C - k_c C T_c \quad (3.6)$$

The first term describes the net proliferation of cancer cells. The second term describes the killing of cancer cells by  $T_c$  cells, which can occur via mechanisms such as granzyme/perforin-induced apoptosis [60], [64].

7. Time evolution of IFN $\gamma$  concentration:

$$\frac{d[IFN\gamma]}{dt} = p_{1-IFN} Th_1 \left( \frac{r_{IL4}}{r_{IL4} + [IL - 4]} \right) \left( \frac{r_{IL6}}{r_{IL6} + [IL - 6]} \right) + p_{c-IFN} T_c - \delta_{IFN} [IFN\gamma] \quad (3.7)$$

The first term describes the secretion of  $IFN\gamma$  by  $Th_1$  cells [58], [59], [63], which is inhibited by IL-4 [65] and IL-6 [59]. The second term describes the secretion of  $IFN\gamma$  by  $T_c$  cells [60], and the third term describes the natural decay of  $IFN\gamma$ .

8. Time evolution of IL-4 concentration:

$$\frac{d[IL - 4]}{dt} = p_{2-4}Th_2 + p_{2-4-6}Th_2 \left( \frac{[IL - 6]}{q_{IL6} + [IL - 6]} \right) - \delta_{IL4}[IL - 4] \quad (3.8)$$

The first term describes the IL-4 secreted by  $Th_2$  cells [58], [59], [63]. The second term describes the additional secretion of IL-4 by  $Th_2$  cells in the company of IL-6 [59], [66]. The third term describes the natural decay of IL-4.

9. Time evolution of IL-6 concentration:

$$\frac{d[IL - 6]}{dt} = p_{2-6}Th_2 + p_{Can-6}C - \delta_{IL6}[IL - 6] \quad (3.9)$$

The first term describes the secretion of IL-6 by  $Th_2$  cells [63]. The second term describes the production of IL-6 by ntigen presenting cells,[59], [67] which is assumed to be directly proportional to the number of cancer cells (term 2). The third term describes the natural decay of IL-6.

10. Time evolution of IL-12 concentration:

$$\frac{d[IL - 12]}{dt} = p_{Can-12}C + p_{1-12}Th_1 - \delta_{IL12}[IL - 12] \quad (3.10)$$

The first term describes the production of IL-12 by DCs, which is also assumed to be directly proportional to the number of cancer cells [67]. The second term describes the further production of IL-12 by  $Th_1$ -activated DCs [68]. The third term describes the natural decay of IL-12.

11. PD-1 concentration and its time evolution:

$$[PD - 1] = \rho \left( Th_1 + Th_2 + T_c \right) \quad (3.11)$$

$$\begin{aligned} \frac{d[PD - 1]}{dt} = & \rho \left( \frac{dTh_1}{dt} + \frac{dTh_2}{dt} + \frac{dT_c}{dt} \right) - \beta_+[PD - 1][PD - L1] + \beta_-[PD - 1 : PD - L1] \\ & - \alpha_+[PD - 1][A] + \alpha_-[A : PD - 1] \end{aligned} \quad (3.12)$$

All activated T-cells, i.e.  $Th_1$ ,  $Th_2$ , and  $T_c$ , express PD-1 [60], [62], so the total concentration of PD-1 is proportional to the sum of the T-cell populations, as indicated by Equation (3.11). For simplification purposes, we assume that the same amount of PD-1 is expressed evenly on all types of T-cells, thus allowing for equal proportionality constants for each T-cell population.

Equation (3.12) describes the time evolution of PD-1. The first three terms describe the change in the PD-1 levels due to changing  $Th_1$ ,  $Th_2$ , and  $T_c$  populations, respectively. The fourth term describes the binding of PD-1 to PD-L1 to form the PD-1:PD-L1 complex, while the fifth term describes the dissociation of this complex [60]. Similarly, the fifth term described the binding of PD-1 to Nivolumab and the sixth term describes its dissociation [62].

12. PD-L1 concentration and its time evolution:

$$[PD - L1] = \lambda \left( Th_1 + Th_2 + T_c + C \right) + \lambda_{Can-IFN} C \left( \frac{[IFN\gamma]}{q_{IFN-PDL1} + [IFN\gamma]} \right) \quad (3.13)$$

$$\begin{aligned} \frac{d[PD - L1]}{dt} = & \lambda \left( \frac{dTh_1}{dt} + \frac{dTh_2}{dt} + \frac{dT_c}{dt} + \frac{dC}{dt} \right) \\ & + \lambda_{Can-IFN} \frac{dC}{dt} \left( \frac{[IFN\gamma]}{q_{IFN-PDL1} + [IFN\gamma]} \right) \\ & - \beta_+ [PD - 1][PD - L1] + \beta_- [PD - 1 : PD - L1] \end{aligned} \quad (3.14)$$

Like PD-1, PD-L1 is also expressed on all activated T cells, i.e.  $Th_1$ ,  $Th_2$ ,  $T_c$  [60], [61]. It is also expressed on cancer cells [60]–[62], leaving the total concentration of PD-L1 proportional, in part, to the sum of the T-cell and cancer cell populations, as indicated by the first four terms in Equation (3.13). We make the same simplifying assumption as before that the PD-L1 expression is evenly distributed across all types of cells. Furthermore, the expression of PD-L1 by cancer cells specifically experiences upregulation by IFN $\gamma$  [60]–[62], which is illustrated by a factor on the fifth term in Equation (3.13).

The time evolution of PD-L1 is described by Equation (3.14). As such, the first five terms describe the change in PD-L1 levels that occur due to changing T-cell and cancer cell populations, owing to the aforementioned proportionality. We simplify the model by assuming that the proteins reach their steady state values instantaneously with respect to the time scale of the changes in cell populations (i.e. the cell division rate) so that  $\frac{d[IFN\gamma]}{dt} \approx 0$ . The seventh term describes the binding of PD-1 to PD-L1,

while the dissociation of the resulting PD-1:PD-L1 complex [60] is described by the seventh term.

13. Time evolution of PD-1:PD-L1 complex concentration:

$$\frac{d[PD - 1 : PD - L1]}{dt} = \beta_+[PD - 1][PD - L1] - \beta_-[PD - 1 : PD - L1] \quad (3.15)$$

The first term describes the formation of the PD-1:PD-L1 complex via the binding of PD-1 to PD-L1, and the second term describes the dissociation of this complex [60].

14. Time evolution of free Nivolumab concentration:

$$\frac{d[A]}{dt} = \tilde{A}(t) - \alpha_+[A][PD - 1] + \alpha_-[A : PD - 1] - \delta_A[A] \quad (3.16)$$

The first term describes the administration of Nivolumab into the system, which can be time-dependent in certain treatment schedules. The second term describes the binding of PD-1 to Nivolumab, thus forming the Nivolumab:PD-1 complex, and the third term describes the dissociation of this complex [62]. We assume that the dissociation constant  $K_\alpha \equiv \alpha_-/\alpha_+ \ll K_\beta \equiv \beta_-/\beta_+$  so that Nivolumab has a higher binding affinity for PD-1 than that of PD-L1, allowing the drug to displace PD-L1 from the PD-1:PD-L1 complex, dismantling it. In simulations, we assume that the rate of association of PD-1 is equivalent for Nivolumab and PD-L1, i.e.  $\alpha_+ = \beta_+$ , which ends up removing a kinetic parameter from the system, as will be seen in the next section. The fourth term in the equation describes the natural decay of Nivolumab.

15. Time evolution of Nivolumab:PD-1 complex concentration:

$$\frac{d[A : PD - 1]}{dt} = \alpha_+[A][PD - 1] - \alpha_-[A : PD - 1] \quad (3.17)$$

The first term describes the binding of Nivolumab with PD-1 to form the Nivolumab:PD-1 complex, and the second term describes its dissociation [62].

### 3.1.2 Modeling recombinant IL12 administration

Logically, the administration of recombinant IL-12 should ideally increase the total IL-12 concentration in the system, directly affecting the time evolution of the populations of

naive helper (CD4+) T-cells, type 1 helper T-cells, and CD8+ cytotoxic T-cells. These effects are described by the following five equations. All other equations remain identical to those presented above in the preceding section.

1. We assume that the initial recombinant IL-12 dose experiences natural decay. Hence, the time evolution of recombinant IL-12,  $[R - IL12]$ , may be described by:

$$\frac{d[R - IL12]}{dt} = -\delta_{R-IL12}[R - IL12], \quad (3.18)$$

where the decay rate is taken to correspond to a drug half-life of 30 hours [69].

2. We then define the total IL-12 concentration,  $[T - IL12]$ , as:

$$[T - IL12] = [R - IL12] + [IL - 12], \quad (3.19)$$

where the time evolution of  $[IL - 12]$  is given in Equation 3.10 of Section 3.1.

Then all instances of IL-12 concentration in the equations for the naive helper (CD4+) T-cells, type 1 helper T-cells, and CD8+ cytotoxic T-cells are replaced by the total IL-12 concentration, resulting in the following equations:

3. Time evolution of naive helper (CD4+) T-cell population:

$$\frac{dT_{N4}}{dt} = n_4 T_{N4} - \left( d_{1-12} T_{N4} \frac{[T - IL12]}{q_{dIL12} + [T - IL12]} \right. \quad (3.20)$$

$$\left. + d_{1-IFN} T_{N4} \frac{[IFN\gamma]}{q_{IFN-1} + [IFN\gamma]} \right) \left( \frac{s_1}{s_1 + [PD - 1 : PD - L1]} \right) - \left( d_2 T_{N4} \frac{[IL - 4]}{q_{dIL4} + [IL - 4]} \right) \left( \frac{s_2}{s_2 + [PD - 1 : PD - L1]} \right) \quad (3.21)$$

4. Time evolution of type 1 helper T-cell population:

$$\frac{dTh_1}{dt} = n_1 Th_1 + \left( d_{1-12} T_{N4} \frac{[T - IL12]}{q_{dIL12}} \right. \quad (3.22)$$

$$\left. + [T - IL12] + d_{1-IFN} T_{N4} \frac{[IFN\gamma]}{q_{IFN-1} + [IFN\gamma]} \right) \left( \frac{s_1}{s_1 + [PD - 1 : PD - L1]} \right) \quad (3.23)$$

5. Time evolution of cytotoxic (CD8+) T-cell population:

$$\frac{dT_c}{dt} = n_c T_c + g_{c-12} T_c \frac{[T - IL12]}{q_{gIL12} + [T - IL12]} + d_c T_{N8} \left( \frac{Th_1}{q_1 + Th_1} \right) \left( \frac{s_c}{s_c + [PD - 1 : PD - L1]} \right). \quad (3.24)$$

## 3.2 Parameters

As shown in the previously displayed equations, this mathematical model relies on several parameters. We provide a description for each of the 47 relevant kinetic parameters in the following table.

Table 3.1: Description of the kinetic parameters in the mathematical model

Name	Description
$n_4$	Net proliferation rate of $T_{N4}$ cells
$n_8$	Net proliferation rate of $T_{N8}$ cells
$n_1$	Net proliferation rate of $Th_1$ cells
$n_c$	IL12-independent net proliferation rate of $T_c$ cells
$n_{Can}$	Net proliferation rate of cancer cells
$g_2$	IL4-independent growth rate of $Th_2$ cells
$g_{2-4}$	IL4-dependent growth rate of $Th_2$ cells
$g_{c-12}$	IL12-dependent growth rate of $T_c$ cells
$\delta_2$	Death rate of $Th_2$ cells
$d_{1-IFN}$	IFN $\gamma$ -dependent differentiation rate of $T_{N4}$ cells into $Th_1$ cells
$d_{1-12}$	IL12-dependent differentiation rate of $T_{N4}$ cells into $Th_1$ cells
$d_2$	IL4-dependent differentiation rate of $T_{N4}$ cells into $Th_2$ cells
$d_c$	Rate of differentiation of $T_{N8}$ cells into $T_c$ cells

$k_c$	Rate of cancer cell killing by $T_c$ cells
$p_{1-IFN}$	Rate of production of IFN $\gamma$ by $Th_1$ cells
$p_{2-4-6}$	IL6-dependent production of IL-4 by $Th_2$ cells
$p_{Can-6}$	Rate of production of IL-6 by antigen presenting cells (assumed proportional to the number of cancer cells)
$p_{Can-12}$	Rate of production of IL-12 by DCs (assumed proportional to the number of cancer cells)
$\delta_{IFN}$	Decay rate of IFN $\gamma$
$\delta_{IL4}$	Decay rate of IL-4
$\delta_{IL6}$	Decay rate of IL-6
$\delta_{IL12}$	Decay rate of IL-12
$\delta_A$	Decay rate of Nivolumab
$q_1$	Half-maximal $Th_1$ cell population for $T_{N8}$ differentiation into $T_c$ cells
$q_{IFN-1}$	Half-maximal IFN $\gamma$ concentration for IFN $\gamma$ -dependent differentiation of $T_{N4}$ cells into $Th_1$ cells
$q_{IFN-PDL1}$	Half-maximal IFN $\gamma$ concentration for IFN $\gamma$ -dependent PD-L1 expression by cancer cells
$q_{gIL4}$	Half-maximal IL-4 concentration for IL4-dependent proliferation of $Th_2$ cell
$q_{dIL4}$	Half-maximal IL-4 concentration for IL4-dependent differentiation of $T_{N4}$ cells into $Th_2$ cells
$q_{IL6}$	Half-maximal IL-6 concentration for IL6-dependent production of IL-4 by $Th_2$ cells
$q_{dIL12}$	Half-maximal IL-12 concentration for IL12-dependent differentiation of $T_{N4}$ cells into $Th_1$ cells
$q_{gIL12}$	Half-maximal IL-12 concentration for IL12-dependent proliferation of $T_c$ cells
$r_{IFN}$	Half-maximal IFN $\gamma$ concentration for IFN $\gamma$ -dependent inhibition of $Th_2$ proliferation

$r_{IL4}$	Half-maximal IL-4 concentration for IL4-dependent inhibition of IFN $\gamma$ production by $Th_1$ cell
$r_{IL6}$	Half-maximal IL-6 concentration for IL6-dependent inhibition of IFN $\gamma$ production by $Th_1$ cells
$\rho$	Per-cell expression level of PD-1
$\lambda$	Per-cell expression level of PD-L1
$\lambda_{Can-IFN}$	IFN $\gamma$ -dependent PD-L1 expression per cancer cell
$\beta_+$	Rate of association of PD-1 and PD-L1
$\beta_-$	Rate of dissociation of PD-1:PD-L1 complex
$\alpha_-$	Rate of dissociation of Nivolumab:PD-1 complex
$s_1$	Half-maximal PD-1:PD-L1 concentration for inhibition of $T_{N4}$ differentiation into $Th_1$ cells
$s_2$	Half-maximal PD-1:PD-L1 concentration for inhibition of $T_{N4}$ differentiation into $Th_2$ cell
$s_c$	Half-maximal PD-1:PD-L1 concentration for inhibition of $T_{N8}$ differentiation into $T_c$ cells
$p_{1-12}$	Rate of IL-12 production by $Th_1$ cells
$p_{2-4}$	Rate of IL6-independent production of IL-4 by $Th_2$ cells
$p_{2-6}$	Rate of IL-6 production by $Th_2$ cells
$p_{c-IFN}$	Rate of IFN $\gamma$ production by $T_c$ cells

We display the numerical values of the parameters and initial conditions for protein levels and relative T-cell populations in the following Table 3.2. Average patient data is represented by the “Nominal value” column and the parameter units can be seen in the “Units” column. Note that the unit “min” denotes a timescale of minutes in an abbreviated form. We also present ranges in the “Range” column for each parameter with the purpose of searching the parameter space with Matlab’s genetic algorithm to match the average patient data. For protein levels and T-cell fractions, the ranges were set by the minimum and maximum experimentally measured values from all patient data. All of these ranges were used during global sensitivity analysis. Additionally, these ranges were

used to simulate virtual patient data for male populations subjected to a 3-day nivolumab treatment schedule. Note that female populations were generated with some of these ranges altered by applying random factors to each end of the range; this is further explained in the following chapter. When using the genetic algorithm to match the average patient data, the T-cell fractions were set to the average of all patients without treatment while protein levels were sampled from a range set within one standard deviation of the average value.

Table 3.2: Values and ranges of the kinetic parameters, initial protein levels, and initial T-cell populations used for virtual patient simulation and local/global sensitivity analysis

Parameter	Nominal value	Range	Units	Reference
$n_4$	$2.9 \times 10^{-2}$	$\ln(2)/20 - \ln(2)$	day <sup>-1</sup>	estimated from [63], [65]
$n_8$	$8.2 \times 10^{-3}$	$\ln(2)/20 - \ln(2)$	day <sup>-1</sup>	estimated from [63], [65]
$n_1$	$7.7 \times 10^{-3}$	$\ln(2)/20 - \ln(2)$	day <sup>-1</sup>	estimated from [63], [65]
$n_c$	$8.3 \times 10^{-3}$	$\ln(2)/20 - \ln(2)$	day <sup>-1</sup>	estimated from [63], [65]
$n_{Can}$	$6.9 \times 10^{-2}$	$\ln(2)/100 - \ln(2)/5$	day <sup>-1</sup>	estimated
$g_2$	$3.7 \times 10^{-2}$	$\ln(2)/20 - \ln(2)$	day <sup>-1</sup>	estimated from [63], [65]
$g_{2-4}$	$3.9 \times 10^{-2}$	$\ln(2)/20 - \ln(2)$	day <sup>-1</sup>	estimated from [63], [65]
$g_{c-12}$	$3.8 \times 10^{-2}$	$\ln(2)/20 - \ln(2)$	day <sup>-1</sup>	estimated from [63], [65]

$\delta_2$	$1.2 \times 10^{-2}$	$\ln(2)/60 - \ln(2)/7$	$\text{day}^{-1}$	estimated from [63], [65]
$d_{1-IFN}$	$7.4 \times 10^{-2}$	$\ln(2)/20 - \ln(2)$	$\text{day}^{-1}$	estimated from [70]
$d_{1-12}$	$7.4 \times 10^{-2}$	$\ln(2)/20 - \ln(2)$	$\text{day}^{-1}$	estimated from [70]
$d_2$	$3.6 \times 10^{-2}$	$\ln(2)/20 - \ln(2)$	$\text{day}^{-1}$	estimated from [70]
$d_c$	$3.7 \times 10^{-2}$	$\ln(2)/20 - \ln(2)$	$\text{day}^{-1}$	estimated from [70]
$k_c$	$3.6 \times 10^{-4}$	$10^{-8} - 10^{-2}$	$T_c \text{ cell}^{-1} \cdot \text{day}^{-1}$	estimated
$p_{1-IFN}$	$8.9 \times 10^{-4}$	$6.5 \times 10^{-4} - 1.7 \times 10^{-2}$	$\frac{\text{pg/mL}}{Th_1 \text{ cell} \cdot \text{day}}$	estimated
$p_{2-4-6}$	$3.9 \times 10^{-4}$	$1.4 \times 10^{-7} - 1.4 \times 10^{-2}$	$\frac{\text{pg/mL}}{Th_2 \text{ cell} \cdot \text{day}}$	estimated
$p_{Can-6}$	$8.9 \times 10^{-3}$	$7.2 \times 10^{-3} - 7.2 \times 10^{-1}$	$\frac{\text{pg/mL}}{\text{cancer cell} \cdot \text{day}}$	estimated
$p_{Can-12}$	$1.3 \times 10^{-6}$	$8.3 \times 10^{-7} - 9.7 \times 10^{-6}$	$\frac{\text{pg/mL}}{\text{cancer cell} \cdot \text{day}}$	estimated from [71]
$\delta_{IFN}$	$7.0 \times 10^{-4}$	$\ln(2)/1000 - \ln(2)/60$	$\text{min}^{-1}$	estimated from [65]
$\delta_{IL4}$	$7.7 \times 10^{-4}$	$\ln(2)/1000 - \ln(2)/60$	$\text{min}^{-1}$	estimated from [65]
$\delta_{IL6}$	$7.0 \times 10^{-4}$	$\ln(2)/1000 - \ln(2)/60$	$\text{min}^{-1}$	estimated from [65]
$\delta_{IL12}$	$4.8 \times 10^{-4}$	$\ln(2)/1440 - \ln(2)/600$	$\text{min}^{-1}$	estimated from [71]
$\delta_A$	$4.7 \times 10^{-2}$	$\ln(2)/15 - \ln(2)/10$	$\text{day}^{-1}$	estimated from [71]
$q_1$	$1.7 \times 10^2$	$1 - 10^5$	$Th_1 \text{ cells}$	estimated

$q_{IFN-1}$	$8.6 \times 10^{-1}$	$10^{-3} - 10^2$	$[IFN\gamma]$ (pg/mL)	estimated
$q_{IFN-PDL1}$	$4.1 \times 10^{-1}$	$10^{-3} - 10^2$	$[IFN\gamma]$ (pg/mL)	estimated
$q_{gIL4}$	1.8	$10^{-3} - 10^3$	$[IL - 4]$ (pg/mL)	estimated
$q_{dIL4}$	$2.4 \times 10^{-2}$	$10^{-3} - 10^3$	$[IL - 4]$ (pg/mL)	estimated
$q_{IL6}$	$1.5 \times 10^2$	$10^2 - 10^4$	$[IL - 6]$ (pg/mL)	estimated
$q_{dIL12}$	$5.0 \times 10^{-2}$	$10^{-3} - 10^2$	$[IL - 12]$ (pg/mL)	estimated
$q_{gIL12}$	2.0	$10^{-3} - 10^2$	$[IL - 12]$ (pg/mL)	estimated
$r_{IFN}$	$2.0 \times 10^{-1}$	$10^{-3} - 10^2$	$[IFN\gamma]$ (pg/mL)	estimated
$r_{IL4}$	3.3	$10^{-1} - 10^3$	$[IL - 4]$ (pg/mL)	estimated
$r_{IL6}$	$1.6 \times 10^2$	$10^2 - 10^4$	$[IL - 6]$ (pg/mL)	estimated
$\rho$	$7.7 \times 10^{-2}$	$10^{-6} - 10^1$	(pg/mL)/T-cell	estimated from [71]
$\lambda$	$1.0 \times 10^1$	$10^{-6} - 10^1$	(pg/mL)/cell	estimated from [71]
$\lambda_{Can-IFN}$	$9.1 \times 10^{-4}$	$10^{-10} - 10^{-1}$	(pg/mL)/cancer cell	estimated from [71]
$\beta_+$	$9.8 \times 10^{-4}$	$1.4 \times 10^{-4} - 1.4 \times 10^{-1}$	$((\text{pg/mL}) \cdot \text{day})^{-1}$	estimated
$\beta_-$	2.5	$1.4 - 1.4 \times 10^2$	$\text{day}^{-1}$	estimated
$\alpha_-$	$1.5 \times 10^{-3}$	$1.4 \times 10^{-3} - 1.4 \times 10^{-1}$	$((\text{pg/mL}) \cdot \text{day})^{-1}$	estimated
$s_1$	$4.5 \times 10^{-3}$	$10^{-3} - 10^5$	$[PD - 1 : PD - L1]$ (pg/mL)	estimated
$s_2$	$9.6 \times 10^{-1}$	$10^{-3} - 10^5$	$[PD - 1 : PD - L1]$ (pg/mL)	estimated
$s_c$	2.2	$10^{-3} - 10^5$	$[PD - 1 : PD - L1]$ (pg/mL)	estimated
$p_{1-12}$	$2.4 \times 10^{-2}$	see text	$\frac{\text{pg/mL}}{Th_2 \text{ cell} \cdot \text{day}}$	–
$p_{2-4}$	$3.1 \times 10^{-3}$	see text	$\frac{\text{pg/mL}}{Th_2 \text{ cell} \cdot \text{day}}$	–

$p_{2-6}$	$3.9 \times 10^1$	see text	$\frac{\text{pg/mL}}{T_c \text{ cell} \cdot \text{day}}$	–
$p_{c-IFN}$	$3.8 \times 10^{-5}$	see text	$\frac{\text{pg/mL}}{T_c \text{ cell} \cdot \text{day}}$	–
<b>Protein</b>	<b>Nominal value</b>	<b>Range</b>	<b>Units</b>	<b>Reference</b>
IFN $\gamma$	0.38	0.18 – 482.31	pg/mL	patient data
IL-12	1.76	1.82 – 11.44	pg/mL	patient data
IL-6	7626.67	149.15 – 35884.0	pg/mL	patient data
IL-4	0.62	0.10 – 61.37	pg/mL	patient data
<b>Cell fraction</b>	<b>Nominal value</b>	<b>Range</b>	<b>Units</b>	<b>Reference</b>
Cancer fraction	0.30	0.1 – 0.9*	–	estimated
TN8 fraction	0.65	0.21–0.97	–	patient data
Tc fraction	0.10	0.0–0.59	–	patient data
CD4+ fraction	0.25	0.01–0.69**	–	patient data
Th1 fraction	$2.0 \times 10^{-3}$	0 – 0.99	–	estimated
Th2 fraction	$7.9 \times 10^{-3}$	0 – 0.99***	–	estimated

\*We assume that the tumor consists of a population of cancer cells and a population of immune cells. Then, corresponding to the nominal values given in Table 3, 81% of the tumor is cancer cells and the remaining 19% is the total immune cell population.

\*\*The total immune cell population consists of naive CD8+ T-cells ( $T_{N8}$ ), CD8+ cytotoxic T-cells ( $T_c$ ), and a population of CD4+ cells, so we always impose the constraint (TN8 fraction + Tc fraction + CD4+ fraction) = 1.

\*\*\*The CD4+ fraction is further subdivided, being comprised of naive helper CD4+ T-cells ( $T_{N4}$ ), type 1 helper T-cells ( $Th_1$ ) and type 2 helper T-cells ( $Th_2$ ). As a result, impose the constraint (Th1 fraction + Th2 fraction + TN4 fraction) = 1 at all times.

Parameters 44-47 do not have a specified range as they were calculated at the beginning of each simulation under the assumption of initial steady state protein levels (Equations (3.7)-(3.10)) using the initial T-cell population values, along with the constraint that all parameters are non-negative. Thus for local and global sensitivity analysis, it was necessary to re-calculate parameters 44-47 for each simulation.

In order to ensure Nivolumab's increased binding affinity for PD-1 compared to that of PD-L1, we imposed the additional constraint stating that parameter 40 < 0.1 parameter 39 for each simulation.

Furthermore, we note that the PD-1 and PD-L1 concentrations were initialized for each simulation according to Equations (3.11) and (3.13), respectively, with the initial cell populations and relevant protein level. In an initial analysis, we used an increased upper bound for the net proliferation rate of cancer cells, parameter 5. This occasionally resulted in nonphysical growth of the cancer population over the three day treatment window in cases of non-response. When this happened, the model output was most sensitive to parameters controlling the CD8+ cytotoxic T-cell population and its efficiency at killing the cancer cells. Important notes regarding fraction parameters are situated below the table.

# Chapter 4

## Sex-related differences in the immune system drive differential responses to anti-PD-1 immunotherapy

### 4.1 Introduction

Immune checkpoint inhibitors (ICIs) have been a promising avenue for cancer immunotherapy in the last few decades. Designed with high affinity for specific membrane-bound receptors, such as PD-1, PDL-1, or CTLA-4 [72], such antibodies block mechanisms that enable cancer cells to evade the anti-tumor activity of T-cells, which in principle, enables the immune system to recognize and kill the malignant cells. Similar to other immunotherapies, the clinical success of ICIs varies greatly among patients and is unpredictable [73], [74], which reflects the impact of patient-specific variability in immune response on treatment success. Immunotherapies targeting the PD-1/PDL-1 pathway have surpassed the 10% response rate ceiling typically associated with other immunotherapies [75], though they are subject to limitations imposed by a patient's specific immune system and tumor microenvironment. Consequently, it is imperative to investigate how variability in the immune system can influence treatment response to better predict therapeutic outcomes for the average patient and to develop strategies for identifying which patients are good candidates for immunotherapy.

Pre-clinical studies and clinical trials using live human subjects are crucial for the development and refinement of dosing regimens for pharmaceutical interventions. However, they are expensive and time consuming to conduct, and they do not necessarily provide

insight into the range of responses that can be exhibited due to patient-specific variability. Systems biology is a cost-effective approach that enables the integration of experimental data with computational and mathematical modeling, allowing for in-depth analysis of the complex interactions that can drive variability in a biological system and lead to differences in treatment response. This is particularly important for the study of how variability in the immune system can affect response to anti-tumor therapies, given the complexity of the immune system resulting from both positive and negative feedback loops between different cell subtypes and signaling molecules.

One major variable in anticancer immunity is sex hormones [76], which exert regulatory effects on both the cancer and immune cell populations [77]. Indeed, sex hormone receptors are over-expressed in many different cancer types, leading to the misregulation of several pathways related to growth and development. In breast tissue, for example, sex steroids sustain the stem cell population (in normal and malignant cells) [78] and they play a key role in the epithelial-mesenchymal transition (EMT) that leads to metastasis and invasion [79]. While the data is limited, it points to estrogen receptor  $\beta$  (ER $\beta$ ) and progesterone receptor (PR) isoforms as the key drivers of these effects, while the role of androgen receptors (AR) remains uncertain [78]. In contrast, in prostate cancer, it is generally accepted that tumor growth is promoted by AR and inhibited by ER $\beta$ , though emerging data suggests that ER $\beta$  may have dual effects [80]. In immune cells, estrogen induces Th2 response and T-cell homing, while androgens, such as testosterone, augment the Th1 response and the activation of CD8+ T-cells, leading to increased production of anti-inflammatory cytokine IL-10 [81]. In our previous work [56], [57], we found significant sex-related differences in patient-derived distributions of cytokine levels and immune cell populations, under both treatment and control conditions. Given the breadth and complexity of these differential regulatory effects, systems biology provides the optimal approach to study how sex-related differences in the immune system drive response dynamics for cancer immunotherapy.

Here we extend our previously-developed systems biology model for anti-PD1 immunotherapy [56], [57], to examine how sex-specific differences in the immune system contribute to variability in the response to treatment. Model simulations are consistent with previous clinical results [82], [83], which showed that, on average, biological male cancer patients experience more favourable outcomes than female patients in response to anti-PD1 immunotherapy. Indeed, due to known basal immune variations between sexes [84] as well as historical exclusion of females from clinical trials [85], it is unsurprising that therapies developed with the male immune system in mind appear to prove less effective in the female population. Thus, results from this in-silico study strengthen the demand for research into the particular immune characteristics that influence the treatment response gap between males and females, which can further inform systems biology-based

and clinical studies aiming to rectify it.

This chapter is outlined as follows. In Section 4.2.1, we describe the development of the mathematical model and simulated treatment protocols for both anti-PD-1 immunotherapy alone and in combination with recombinant IL12. We detail the integration of established immune cell interactions with ex-vivo data sampled from a cohort of patients with head and neck squamous cell carcinoma. To this end, we first outline the literature review that was conducted to understand the known differences in the immune system between males and females. Then, in Section 4.2.2 we describe how these differences were incorporated into the mathematical model by changing key model parameters. We further describe how parameter sets representing “male” and “female” virtual patients were generated via Latin hypercube sampling. Afterwards, we provide greater detail for the simulation of combination therapy with recombinant IL12 in Section 4.2.3. Following simulations of anti-PD-1 immunotherapy, sex differences among the patient populations in the basal immune system are discussed in Section 4.3.1 and in Section 4.3.2, we assess the efficacy of the treatment as the percentage of the virtual populations that responded favorably to treatment for both male and female virtual populations. In Section 4.3.3, we further investigate the differences between male and female virtual populations in response to combination therapy with anti-PD-1 immunotherapy and recombinant IL12. Finally, in Section 4.4, we conclude with a discussion of the results of the study and their implications for developing personalized approaches to immunotherapy.

## 4.2 Methods

### 4.2.1 Systems biology approach

In previous work [56], [57], we developed a multi-scale network describing the interactions between key immune cell subtypes and cytokines that are relevant to immunotherapies targeting PD1 receptors. This mathematical model was parameterized using a combination of literature data and temporal measurements of T-cell populations and cytokine secretion observed in a live ex-vivo human system obtained from biopsies of patients with head and neck squamous cell carcinoma (HNSCC). The mathematical model is comprised of 17 coupled ordinary differential equations and a total of 47 kinetic parameters. These equations were solved using the MATLAB ode15s solver (R2024a). Described by the pathway shown in Figure 4.1, with five key T cell populations and four cytokines that are critical to the differentiation and activation of T helper cells, the model was used to

simulate a 72 hour treatment protocol in which 132  $\mu\text{g}/\text{mL}$  of nivolumab was administered at  $t = 0$  h,  $t = 24$  h, and  $t = 48$  h with drug washout between each dose.

Patient parameter sets were generated using Latin hypercube sampling (LHS), with bounds supported by the literature, where possible, and the ex-vivo data. Following nivolumab treatment simulation, each patient parameter set was given a “Class” value of 1 or 0, respectively, indicating response or nonresponse to the therapy. The Class of the patient parameter set was determined empirically by comparing the number of cancer cells after the three day dosing schedule to the number of cancer cells after three days of no treatment. Specifically, the treatment was considered a success if the number of cancer cells on day three with treatment was less than the number of cancer cells after three days with no treatment, meaning that the treatment had slowed the tumor growth; in this case the given patient parameter set was deemed a responder. We note that patient parameter sets which experienced cancer regression after 3 days of no treatment were excluded from this analysis so as to avoid inflation of response rates within a patient population. It is conceivable that, within the responder Class, there may be several subsets of response types. For example, some parameter sets might lead to a partial response, where the treatment minimally slows the tumor growth compared to the untreated case. For other parameter sets, there may be a more complete response, where the treatment actually causes cancer cell regression. As a result, it is important to note that many patients deemed responders may still have an increased cancer cell count after treatment compared to before.

Creating virtual patient populations consisting of several hundred or thousands of patients enabled the examination of how variability in immune parameters affect the response to therapy. The assessment of the overall efficacy of the therapy for a particular population was performed by calculating the proportion of responders among the patients; this was referred to as the response rate of the given nivolumab therapeutic session.

## 4.2.2 Generating male and female virtual patient populations

For several years, researchers have explored the differences and similarities between the male and female human immune systems. Notably, differences in T-cell populations and function [86], [87], as well as cytokine production [88]–[90], have been reported between the sexes. Furthermore, clinical data has revealed that 55% of males have an inverted CD4:CD8 ratio (i.e.  $< 1$ ) as opposed to just 44% of females [91]. As another example, female lung cancer patients have, on average, a higher serum sPD-1 level of 105.3 pg/mL, compared to 75.17 pg/mL in their male counterparts [88]. To ensure that sex-specific differences were properly reflected in the model, data and knowledge from the literature were carefully

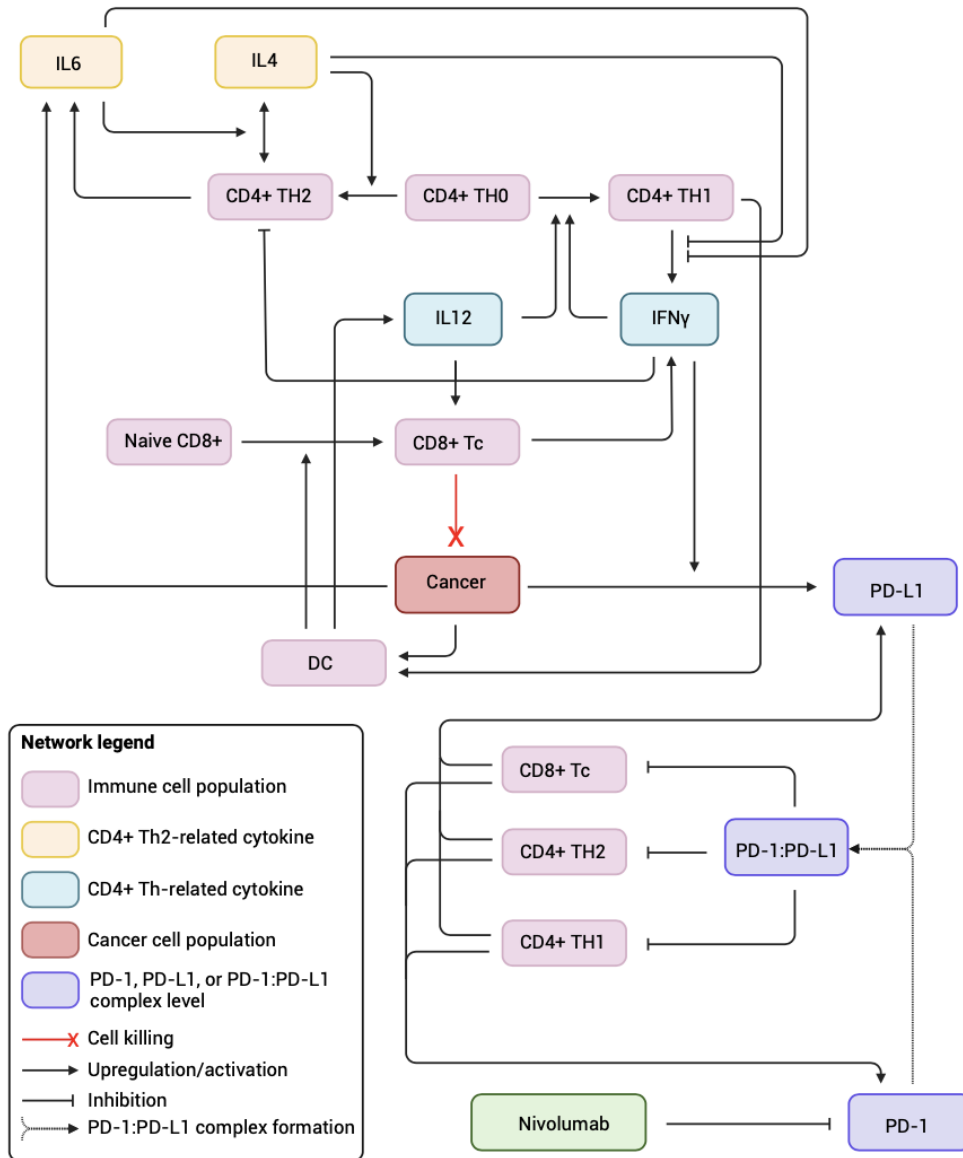


Figure 4.1: Molecular pathway for the previously established systems biology model used in this study. It displays interactions between immune cell populations of CD4+  $T_{H0}$ ,  $T_{H1}$ , and  $T_{H2}$  cells, CD8+ naive and cytotoxic T-cells, cytokines IL4, IL6, IL12, and IFN $\gamma$ , dendritic cells, cancer cells, and PD-1 and PD-L1.

compared with model parameters, enabling the identification of parameters that are likely to be sex-specific and could be leveraged to capture expected differences between male and female patients. The sex-specific differences captured by the model, along with the specific parameters that were altered to capture these differences, are summarized in Table 4.1.

To efficiently generate sex-specific patient parameter sets for further simulation and analysis, we built on the results from prior work [56], [57], where a global sensitivity analysis identified the model parameters that most highly impact the treatment response rate. Specifically, we cross-referenced the most sensitive model parameters with those that are expected to exhibit sex-specific differences, Table 4.1, to pinpoint a subset of parameters,  $\Omega$ , that were both influential on the model response rate *and sex-specific*. We then altered the sampling ranges for this subset of parameters to generate sex-specific parameter sets, representing male and female virtual patient populations, such that the difference in response rates between the virtual populations was similar to what is observed clinically. In particular, parameter sets generated via Latin hypercube sampling using the nominal parameter ranges, see Supplementary Table 3 [57], were taken to represent the male virtual populations. The goal was then to alter the sampling ranges appropriately to generate female virtual populations that exhibited  $\approx 10 - 15\%$  lower response rate, while keeping the parameters within biologically-relevant ranges [82], [83]

This was accomplished as follows. First, the sampling range for each parameter in Table 4.1 was individually subjected to a significant increase with respect to its nominal range, a virtual population of 1000 was generated via LHS, and the change in the response rate, relative to the nominal sampling range, was noted. Next, the sampling range for each parameter in Table 4.1 was individually subjected to a significant decrease with respect to its nominal range, and the response rate of the corresponding virtual population was noted. This was repeated for each individual parameter in the Table 4.1. In addition, the analysis was repeated for different factors applied to the sampling ranges, with the aim of identifying the degree that each sampling range must be altered to produce a significant change in the response rate compared to the nominal sampling range (i.e. virtual male population), as well as the directionality of the change. We observed that an increase or decrease by a factor of 50, that is, either a multiplication or a division of the nominal parameter sample range by 50, proved sufficient in providing insight into the sensitivities of kinetic parameters. For example, a 50-fold increase in the sampling range for the net proliferation rate of  $T_{H1}$  cells, while keeping all other parameter sampling ranges unaltered, led to a response rate that was roughly 19% lower than the virtual male population.

Due to the different natures of the parameters, not all of the parameters in Table 4.1 could simply be altered by multiplying or dividing their sampling ranged by 50. Specifically, some of the parameters correspond to a fraction of a total number of cells, and thus are

Table 4.1: Sex-specific differences in basal immune system reported in the literature and associated model parameter(s) that were modified to capture the respective sex difference

Sex difference	Associated parameter(s) name (description)	Reference
Increased IFN $\gamma$ production by CD4+ T cells in females	$p_{1-IFN}$ (rate of production of IFN $\gamma$ by $Th_1$ cells)	[87]
Higher activated and proliferating CD4+ T cells in females	$n_4$ (net proliferation rate of $T_{N4}$ )	[86]
Higher activated and proliferating CD8+ T cells in females	$n_8$ (net proliferation rate of $T_{N8}$ ), $n_c$ (IL12-independent net proliferation rate of $T_c$ cells)	[86]
Higher PD-1 expression on CD4+ T cells in females	$\rho$ (per-cell expression level of PD-1)	[88]
Higher PD-1 expression on CD8+ T cells in males	$\rho$ (per-cell expression level of PD-1)	[90]
High PD-L1 expression more likely on female tumors than male	$\lambda$ (per-cell expression level of PD-L1), $\lambda_{Can-IFN}$ (IFN $\gamma$ -dependent PD-L1 expression per cancer cell)	[89]
Increased $Th_2$ functions in females	$p_{2-4}$ (rate of IL6-independent production of IL4 by Th2 cells), $p_{2-6}$ (rate of IL6 production by Th2 cells)	[86]
Increased $Th_1$ functions in males	$n_1$ (net proliferation rate of $T_{H1}$ cells)	[86]
Higher IFN $\gamma$ production by CD8+ in females	$p_{cIFN}$ (rate of IFN $\gamma$ production by $T_c$ cells)	[90]
Increased CD8+ cytotoxic activity in females	$d_c$ (rate of differentiation of $T_{N8}$ cells into $T_c$ cells)	[86]
Higher CD4:CD8 ratio in females	Tc fraction (fraction of T cells that are cytotoxic)*, TN8 fraction (fraction of T cells that are CD8+ naive)*	[91]

defined as a value between 0 and 1. For this case, the sampling range was increased by raising just the lower bound of the sampling range to be arbitrarily close to the upper

bound. Similarly, the sampling range was decreased for such parameters by lowering the upper bound of the sampling range to be arbitrarily close to the lower bound. For example, for any given fractional parameter, let  $l$  be the nominal lower bound from which it is sampled and  $u$  be the nominal upper bound such that  $0 \leq l < u \leq 1$ . If we wanted to sample from a new range that is the bottom 10% of the original range, the lower and upper bounds of the new range, denoted  $l_b$  and  $u_b$ , would be calculated as follows:

$$\begin{aligned} l_b &= l \\ u_b &= 0.1 \times u \end{aligned} \tag{4.1}$$

Similarly, a new range  $[l_t, u_t]$  where  $0 \leq l_t < u_t \leq 1$  indicating the upper 10% of the nominal range  $[l, u]$  would be defined by:

$$\begin{aligned} l_t &= u - 0.1 \times (u - l) \\ u_t &= u \end{aligned} \tag{4.2}$$

As the lower and upper 10% of a range was deemed sufficiently dramatic for a single-parameter sensitivity analysis, the LHS bounds of the fraction parameters were each subjected to changes detailed in equations 4.1 and 4.2, seeking the aforementioned 10 - 15% effect on response rate.

Parameters that satisfied the required effect on the response rate when altered dramatically in accordance to their given parameter type were then deemed suitable for inclusion in the subset  $\Omega$ , designating them as both sex-specific and pivotal to the response rate. With  $\Omega$  cemented, the generation of female patient sets could begin. Unfortunately, little empirical data exists in the literature that can be used to identify distinct ranges of kinetic parameters for male and female virtual patients with a high degree of confidence. Non-identifiability in the model structure further compounds this limitation. Consequently, the approach used in this work focused on generating pseudo-random parameter sets that could accurately recapitulate the difference in response rate to anti-PD-1 immunotherapy that is observed between male and female patients in clinic [82]. To this end, the patient parameter sets that were obtained by sampling the ranges reported in Ref. [57] were taken to represent virtual male patients, and female virtual patient populations were obtained by altering the sampling ranges for the parameters in  $\Omega$ . To accomplish this, a randomly generated factor was generated for both LHS bounds of each and every sex-specific parameter. Every one of these factors was used to either multiply or divide its particular bound for all parameters simultaneously, depending on the directionality of the sex difference. Due to the general absence of knowledge regarding particular ratios between the parameters in the male and female immune system, the random factors were kept within minimal ranges

such as to not overstate the sex differences. While prior experimentation with individual parameter sensitivity used relatively large factors to induce significant change in response rate, altering multiple parameters together allows for an arrival to the desired effect via much more modest adjustments, with random factors not exceeding 3.0.

For example, let parameters  $x, y \in \Omega$  be sex-specific parameters such that the female immune system exhibits higher  $x$  values and lower  $y$  values compared to males. Let  $0 \leq l_x < u_x$  be the nominal (male) lower and upper LHS bounds for  $x$ , and  $0 \leq l_y < u_y$  be the nominal lower and upper LHS bounds for  $y$ . Supposing the random factor to be applied to the parameters must be between  $m$  and  $n$  such that  $1 < m < n$  and  $m, n \in \mathbb{R}$ , the female LHS bounds for  $x$  and  $y$  are determined using the  $rand()$  function in MATLAB [92]. When given an input  $i \in \mathbb{R}$ ,  $rand(i)$  will output a random number between 0 and  $i$ . Thus, a random number between  $m$  and  $n$  would be

$$m + rand(n - m) \tag{4.3}$$

Then, the lower and upper LHS bounds for  $x$ , denoted by  $l_{xf}$  and  $u_{xf}$  respectively, would both be calculated by multiplying their male counterpart by said random factor as represented by the equation below.

$$\begin{aligned} l_{xf} &= (m + rand(n - m)) \times l \\ u_{xf} &= (m + rand(n - m)) \times u \end{aligned} \tag{4.4}$$

Conversely, since  $y$  represents a parameter with decreased values in females compared to males, the new LHS bounds  $l_{yf}$  and  $u_{yf}$  would instead be calculated by dividing the equivalent nominal bounds by a randomly generated factor, as illustrated by the following equation.

$$\begin{aligned} l_{yf} &= \frac{1}{(m + rand(n - m))} \times l \\ u_{yf} &= \frac{1}{(m + rand(n - m))} \times u \end{aligned} \tag{4.5}$$

We note that the  $rand()$  function was run for each bound of every parameter individually, generating a unique output every time. Thus it should be noted that the factors multiplying  $l$  and  $u$  to create  $l_{xf}, u_{xf}, l_{yf}$ , and  $u_{yf}$  are all distinct from one another.

Finally, female patient populations were generated by applying the changes described above to every upper and lower LHS bound associated with a parameter in the subset  $\Omega$ , with each bound impacted in accordance to the sex difference described in Table 4.1

by a unique randomly generated factor. All randomly generated factors were limited to the same bounds for every kinetic parameter in a given population. Due to uncertainty regarding specific female parameter values in relation to the nominal (male) parameter set, multiple female populations were generated using six ranges in which the random factor for alteration of kinetic parameters would be generated. In order of decreasing modesty, these ranges include 1.0-2.0, 1.1-2.5, 1.1-3.0, 2.0-2.5, 2.0-3.0, and 2.5-3.0. Each of these ranges were able to produce favourable results in regards to the 10-15% difference in response rate. Furthermore, fraction parameters were also altered in various fashions to further increase the range of intensity by which the female parameters differ from male. Consisting of just the CD8+ naive T-cell fraction (TN8) and the CD8+ cytotoxic T-cell fraction (Tc), the fraction parameters experience alterations limiting both parameters to the bottom 80% of their respective nominal sampling ranges, and then both to the bottom 50%. Further extreme effects were experimented with by only applying lowered ranges to the CD8+ naive % since literature appears to suggest lower response rate in females, starting with the bottom 50%, then the bottom 10%, and finally the bottom 5% of the nominal sampling range. Altogether, a total of 30 female populations of 1000 patients each were generated for this analysis, as well as one male (defined with unaltered parameter sampling ranges) population of 1000 patients, one male population of 50,000 patients, and one “very” female population of 50,000 using the most extreme alterations on the fraction and the kinetic parameters.

### **4.2.3 Simulating recombinant IL12 + nivolumab combination therapy**

The administration of recombinant IL12 (RIL12) may be an ideal accompaniment to nivolumab in a combination therapy with the aim of increasing efficacy. As a result, we focused our analysis on patients who were classified as nonresponders in simulations of nivolumab treatment alone, examining the rate of conversion of nonresponders into responders following in-silico doses of RIL12 combination therapy. Thus, our investigation depended on the virtually generated populations of patients who had undergone a typical nivolumab treatment regimen, specifically the Class identifier indicating each patient as a responder or nonresponder.

From there, all nonresponders identified via the aforementioned Class were extracted for examination and compiled in ascending order of the final cancer cell count after the 72 hr nivolumab treatment protocol. That is, the nonresponders were organized according to how close they were to responding to nivolumab and thus how likely they would be to respond

to the combination therapy. The top 100 nonresponders from this ordered list were then selected to undergo combination therapy simulations. Nearly identical to the nivolumab simulations, the combination therapy simulations included a dose of RIL12 administered prior to the first dose of nivolumab. After applying the combination treatment to each of the top 100 nonresponders, the percentage of those who responded to the combination treatment was calculated; this value was treated as a conversion rate from nonresponders to responders and gauged the efficacy of combination therapy with RIL12 on the patient population. Conversions were treated similarly in this analysis as response in the nivolumab monotherapy analysis, in that response to combination therapy was defined by a decreased rate of cancer cell growth compared to an untreated case. In this regard, RIL12 combination treatment simulations included a simulation for each patient in which they went an amount of time with no treatment whatsoever; this time was the same as the total treatment time for the combination therapy and thus depended on the administration time. The final cancer cell count was recorded and used for Class determinations where the ratio of the number of cancer cells after treatment to the number of cancer cells after the same timeframe with no treatment was compared to 0.995.

## 4.3 Results

### 4.3.1 Sex-specific differences in basal immune system

Following the sensitivity analysis described in Section 4.2.2, a total of nine parameters were determined to be both sex-specific and influential on the response rate and thus comprise the subset  $\Omega$ . Evidently, some parameters from Table 4.1, such as  $p_{1-IFN}$  and  $p_{2-4}$ , were deemed insufficiently sensitive via sensitivity analysis and thus excluded from  $\Omega$  and therefore the sex-based parameter changes. In Figure 4.2, we plot the distribution of these parameters for populations of 1000 male and 1000 female virtual patients. As indicated in the boxplots in Figure 4.2, both the average value and range of each parameter are distinct between male and female virtual populations, and they follow the trends reported in the literature. For example, the parameters  $n_4$  and  $n_8$ , representing proliferation of CD4+ and CD8+ naive T-cells respectively, are higher in value in the female virtual population than the male, which is consistent with higher CD4+ and CD8+ T-cell female activity [84]. Similarly, higher CD8+ cytotoxic activity [86] is captured in female virtual patients compared to male virtual patients via increased values of parameters  $n_c$  and  $d_c$  in females, which are, respectively, the IL12-independent proliferation rate of cytotoxic T-cells and the rate of differentiation of CD8+ naive T-cells into cytotoxic T-cells. The CD4:CD8

ratio has also been reported to be higher in female patients than male patients [84]. This difference is captured in simulated patients by enforcing lower fractions of TN8 and Tc cells at baseline in female patients, which together comprise the fraction of T-cells that are CD8+ as opposed to CD4+. Finally, the per-cell expression of PD-1 and PD-L1 in male and female virtual patients follows the trends observed in literature. Specifically, high PD-L1 expression is observed more frequently in tumors originating from female patients [89], which is consistent with the trends for  $\lambda$  in Figure 4.2. On the other hand, while the expression of PD-1 is generally higher on female CD4+ T-cells [88] and male CD8+ T-cells [90], the dominance of CD4+ and CD8+ T-cell activity in females, as discussed above, leads to a small overall increase in  $\rho$ , the per-cell PD-1 expression, in female virtual patients.

### 4.3.2 Sex-specific responses to nivolumab

The response rates to the 72-hour nivolumab treatment protocol were recorded for one male and 30 female virtual populations, each comprised of 1000 patients, for a sex-based comparison. In general, female populations that were generated with the distributions of parameters depicted in Figure 4.2 proved less responsive to the male population, which showed a response rate of approximately 56% in simulations. In this work, the response rate was defined as the percentage of the total virtual population that was flagged as a responder to the 72-hour nivolumab treatment protocol. As displayed in Figure 4.3, female populations with minimal changes to the sampling ranges for parameters in  $\Omega$  exhibited a fairly large decrease in response to nivolumab, thus appearing to uphold the male bias in immunotherapy response as reported in the literature [82], [83]. Female populations generated with more extreme differences the sex-specific parameters  $\Omega$  exhibited even larger decreases in the response rate, with some populations having response rates as much as 20% lower than the male virtual population.

As discussed in Section 4.2.1, we distinguished responders from nonresponders by comparing the ratio of the number of cancer cells after the 3 day nivolumab treatment schedule to the number of cancer cells after 3 days of no treatment. In this sense, we are allowing patients to be deemed responders as long as the treatment sufficiently slows the rate at which the cancer cell population increases over time, and does not take into account whether or not the cancer actually regressed. This phenomenon is visualized in Figure 4.4 where histograms were created of the ratio of the number of cancer cells after the 3-day nivolumab treatment to the initial number of cancer cells. In both male and female populations of approximately 1000 patients, it is quite clear that for most of the patients who were determined to have responded to the treatment (particularly seen in Figures 4.4A and

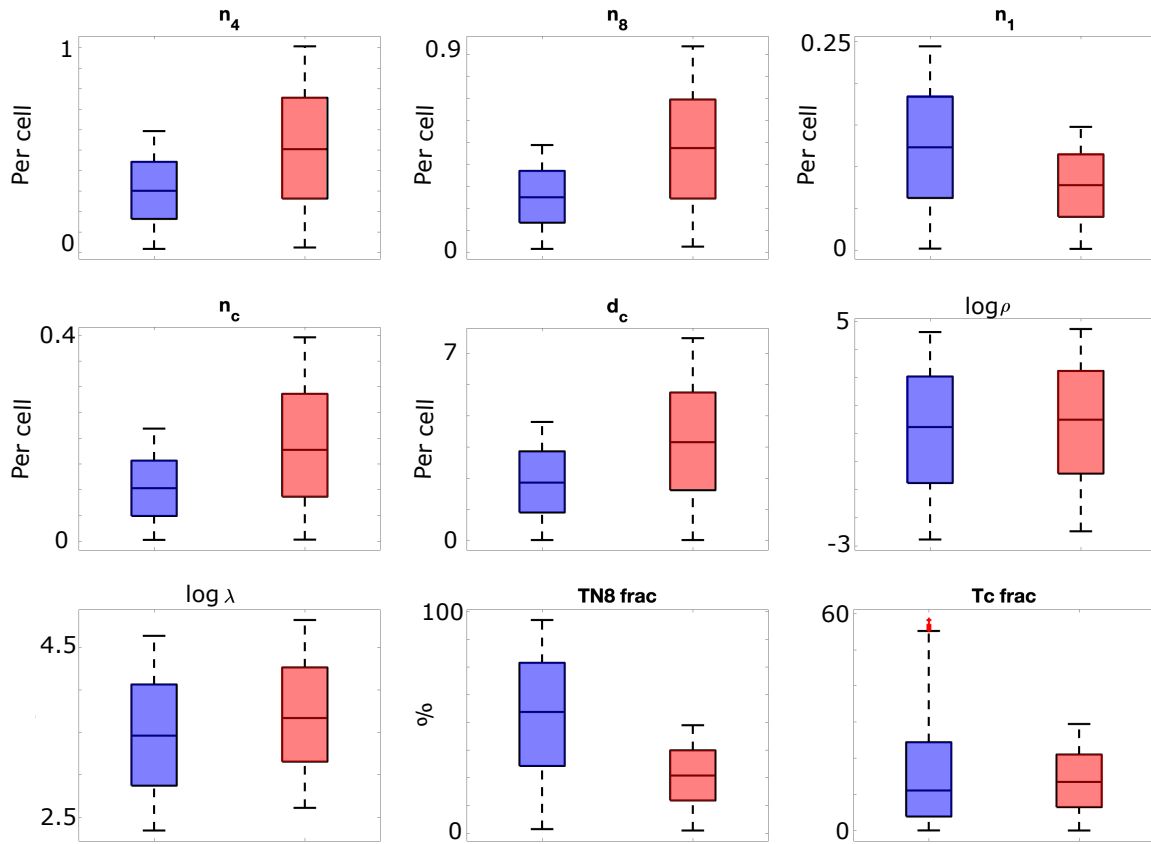


Figure 4.2: Box plots demonstrating the differences between male (blue) and female (red) virtual patients for each parameter in the subset  $\Omega$ . The male virtual patient population was comprised of 1000 patients with parameters generated via Latin hypercube sampling of parameters from the ranges summarized in Supplementary Table 3 [57]. The female virtual patient population was comprised of 1000 patients generated via Latin hypercube sampling of parameters, with the ranges of the parameters in  $\Omega$  altered to represent the ranges expected for female patients. Specifically, parameters that do not represent a fractional cell count were multiplied by a random number between 1.1-2.0, generated individually for each parameter; while the naive and cytotoxic CD8+ T-cell fractions were limited to the bottom 50% of the sampling range used for male patients. For parameters  $\rho$  and  $\lambda$ , the log (base 10) of the parameter values are depicted.

4.4C), this ratio was above 1, indicating an overall increase in the cancer cell population following treatment. It is thus important to note that under a stricter responder definition

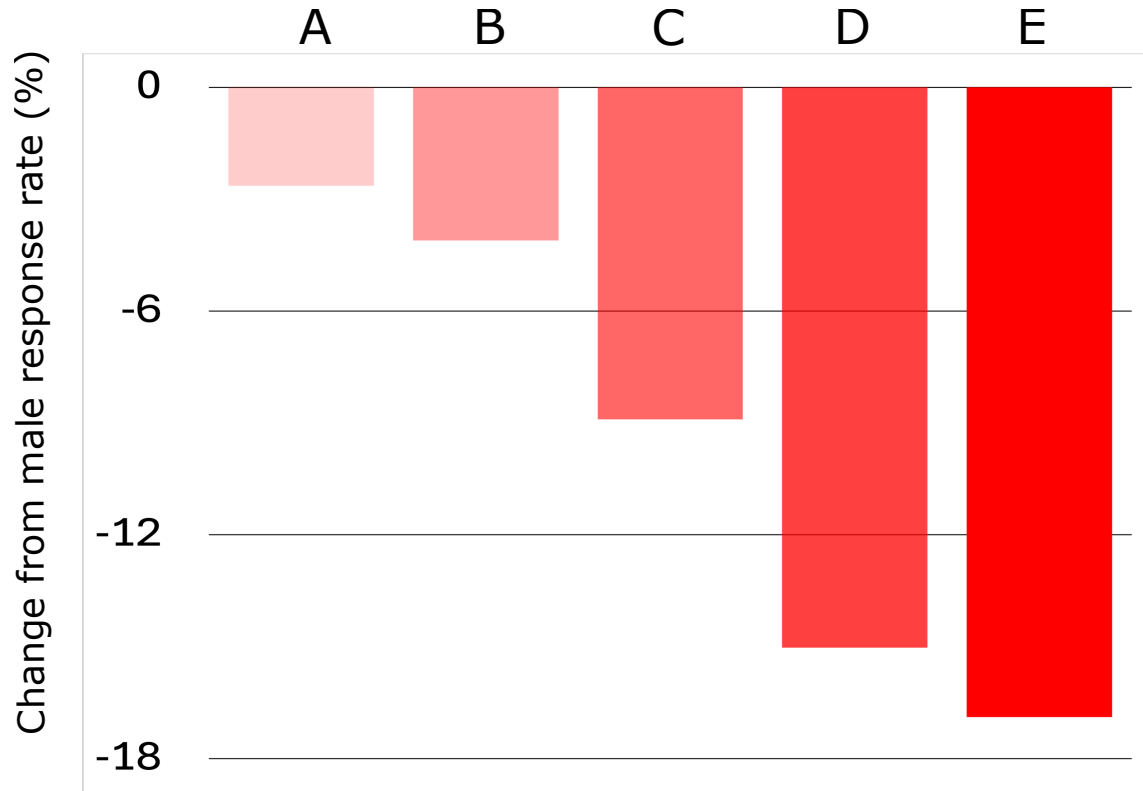


Figure 4.3: Difference in response rate for several female virtual patient populations (A-E) compared to the reference male population. All female populations were generated by multiplying the lower and upper bounds of the sampling ranges for each non-fraction sex-specific kinetic parameter in  $\Omega$  by random factors in the range  $[1.1, 2.0]$ . The different populations were generated by sampling the initial naive CD8+ T cell and CD8+ cytotoxic T cell populations from different ranges. Specifically, population A was generated with the CD8+ naive % and CD8+ cytotoxic % both confined to the bottom 80% of their LHS bounds. Population B features the same parameters further confined to the bottom 50% of the LHS bounds. For populations C, D, and E, only the CD8+ naive %LHS range was lowered to the bottom 50%, 10%, and 5% respectively whilst the CD8+ cytotoxic % remained unaltered as in the male population.

demanding regression of the cancer cell count after treatment, the response rates previously indicated would likely be much lower. Indeed, populations of 1000 male and 1000 female

(specifically as described in Figure 4.2) patients exhibited response rates of 13% and 11% respectively when generated using this definition of the responder in which the ratio of the number of cancer cells after treatment to the initial number of cancer cells must not exceed 0.995.

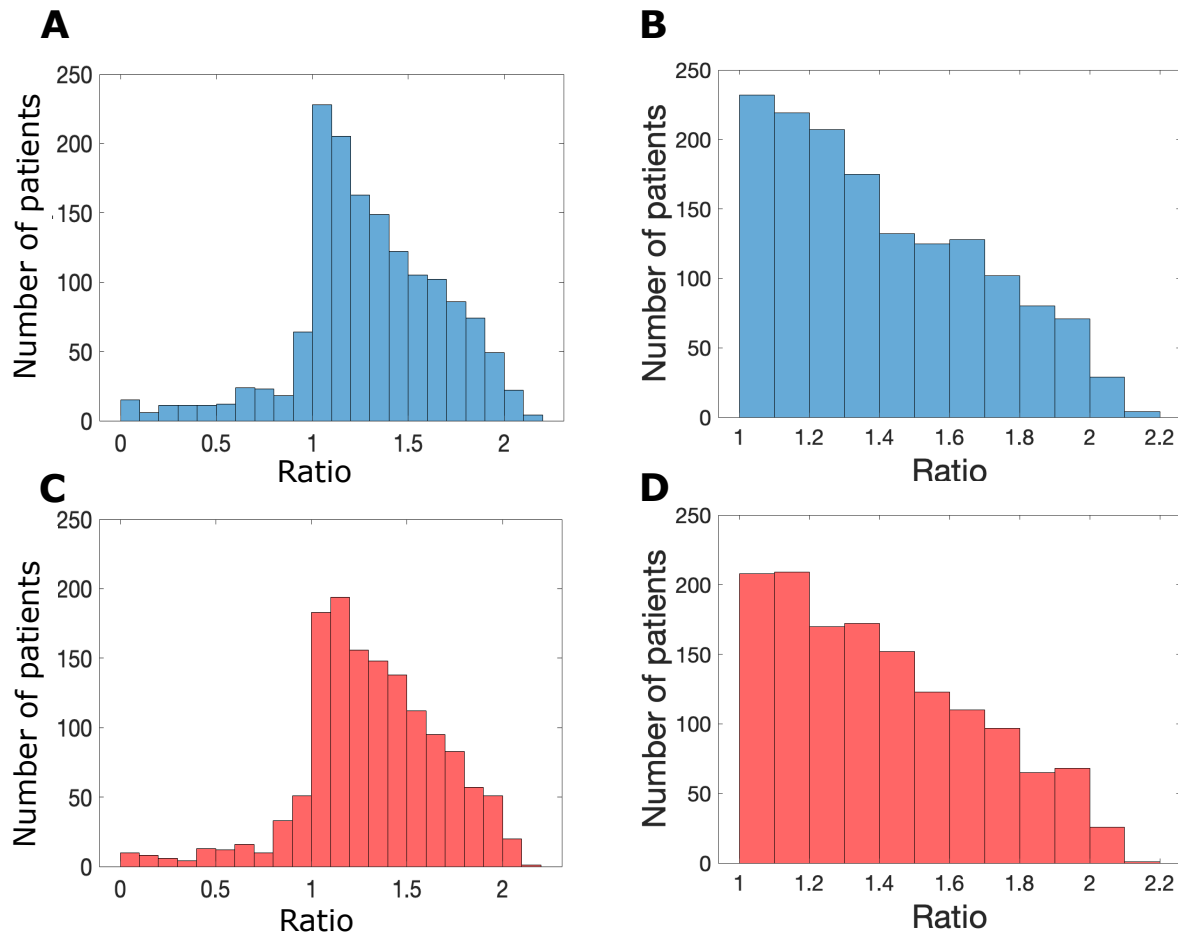


Figure 4.4: Histograms of the ratio of cancer population after treatment vs initial cancer cell count - just putting these here for now. A: male responders, B: male nonresponders, C: female responders, D: female nonresponders. Female population was generated with sex-related alteration factors in the range [1.1, 2.0] with naive and cytotoxic T-cell fractions limited to the bottom 50% of the original range. Both male and female populations comprise of approximately 1500 patients each.

### 4.3.3 Success of simulated recombinant IL12-nivolumab combination therapy depends on patient sex

We previously found [57] that combination treatment with recombinant IL12 (RIL12) administered prior to anti-PD1 immunotherapy could improve the response rate compared to anti-PD1 immunotherapy alone. Here we analyzed whether male and female virtual patient populations exhibit different responses to this combination treatment and whether the optimal sequencing of the drugs depends on patient sex. In an attempt to capture a high degree of patient variability, during this analysis we generated large populations of 50,000 virtual patients for each sex. Due to a general lack of knowledge regarding the impact of patient sex on the efficacy of recombinant IL12, we sought to exaggerate the sex-specific differences between the male and female patient populations. To this end, during the analysis, the nominal parameter ranges were used to generate the male population; to generate the female population, the lower and upper bounds for sampling the sex-specific kinetic parameters in  $\Omega$  were scaled by random factors in the range [2.5,3.0], and the TN8 fraction sampling range was restricted to the bottom 5% of its nominal range. We note that the male and female populations used for this analysis exhibited response rates of 54.69% and 33.08% respectively in regards to the 3-day nivolumab monotherapy treatment schedule. With the female response rate approximately 21% lower than the male response rate, these larger simulations align well the results discussed in Figure 4.3, indicating that both larger and smaller population sample sizes provide grounds for a cohesive study across both mono- and combination therapy analyses.

After both populations of patients were generated via Latin hypercube sampling, they were subjected to several combination treatment scenarios to elucidate the impact of the duration of pre-treatment with recombinant IL12 on the nivolumab treatment response. In the simulations, a dose of 10 pg/mL RIL12 was administered for different pre-treatment windows before nivolumab administration, and the results for both patient populations suggested the increase in efficacy is approximately proportional to the length of the pre-treatment window, see Figure 4.5. Indeed, while the treatment managed to convert about 50% of males and almost 60% of females when administered at the same time as nivolumab, these figures rose to about 60% and 70% respectively when RIL12 was administered 24 hours prior to nivolumab.

These results appear to suggest that female patients may benefit from RIL12-nivolumab combination therapy moreso than their male counterparts. Moreover, the results are further supported by examining the temporal evolution of cancer cell counts in male and female patients during the combination treatment, which are depicted in Figure 4.6. In this figure, blue curves correspond to patients who converted to responders, while red curves

correspond to those who did not. The plots indicate that an apparent lack of conversion to responders pairs with generally milder decreases in cancer cell counts, as observed within the male population. In contrast, the female populations showed a much higher proportion of nonresponders converted into responders, which paired with a generally larger decline in cancer cell counts.

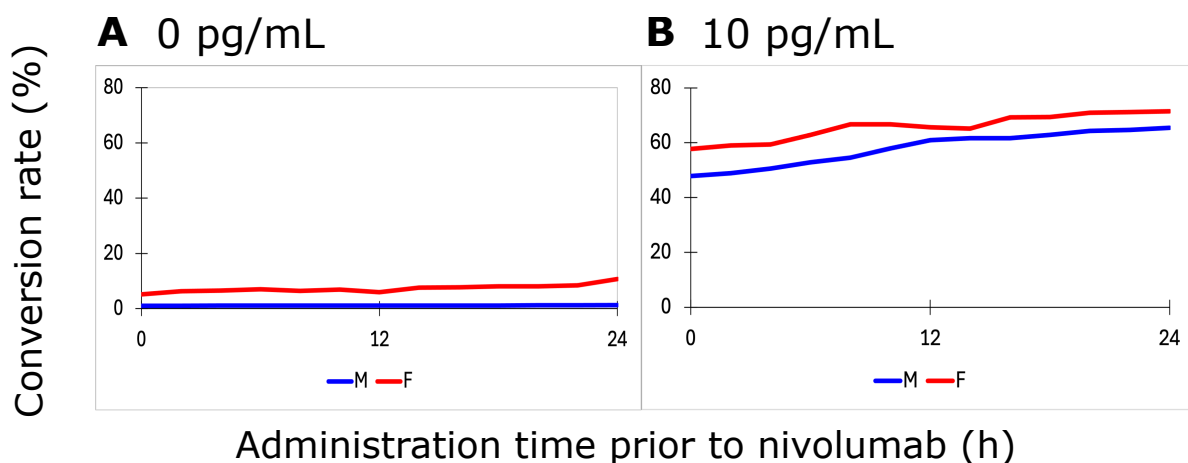


Figure 4.5: Recombinant IL12 simulations for male (M) and female (F) patient populations with administration times up to 24h prior to nivolumab. A: RIL12 dose of 0 pg/mL. B: RIL12 dose of 10 pg/mL. Conversion rate refers to the percentage of nonresponders to nivolumab alone who converted to responders following the addition of simulated RIL12 to the treatment schedule. Male patient results are denoted by the blue line, female patient results are denoted by the red line.

To precisely isolate and understand the effect of recombinant IL12 on the system, simulations were performed with a dose of 0 pg/mL RIL12 at the same administration times as in the preceding analysis. In other words, the system was left to evolve in the absence of drug for a fixed pre-treatment window prior to the administration of nivolumab treatment. The percentages of non-responders that were converted into responders are plotted in Figure 4.5A, comparing the effects of what is essentially a delay in nivolumab treatment on male and female patient populations. Interestingly, this time delay appeared to have a slightly positive effect on the conversion rate of non-responders to responders in both sexes, with females again experiencing the higher benefit. Comparing to figure 4B, which displays the results of 10 pg/mL RIL12 at the same time points for the same male and female populations, it seems that a small number of the non-responders who converted

into responders with combination therapy may have also experienced a decreased cancer cell growth rate by postponing nivolumab monotherapy administration. This may be due to complex dynamics involving T-cell proliferation and the time evolution of cancer cells.

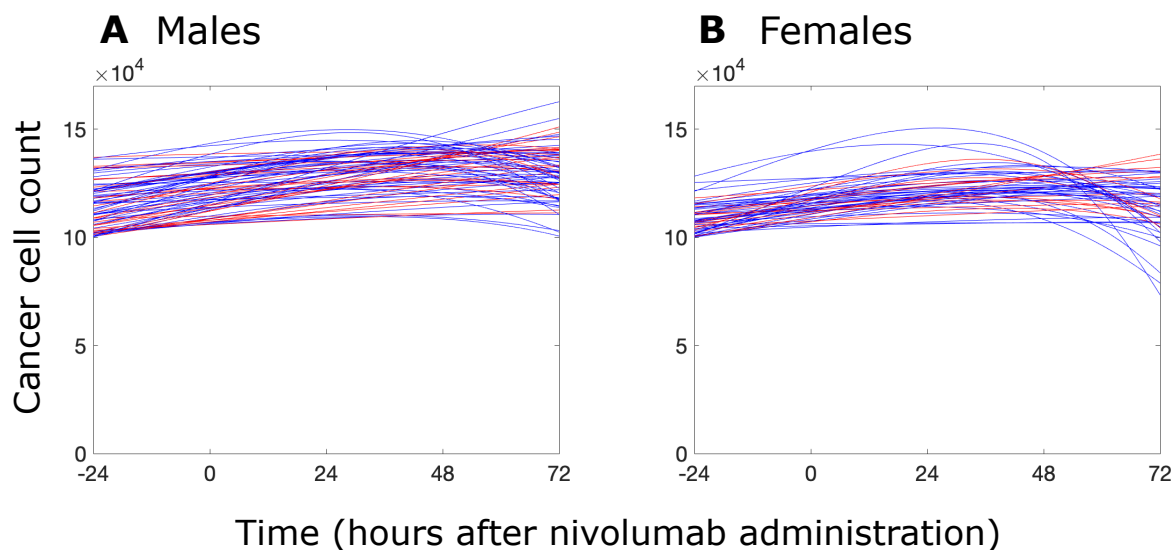


Figure 4.6: Simulated patient cancer cell counts in response to recombinant IL12 administered 24 hours prior to nivolumab. Graph A represents cancer cell count in a virtual population of 50,000 male patients and graph B represents the same for a virtual population of 50,000 female patients. In both graphs, the blue curves represent nonresponders who had successfully converted to responders with the combination treatment, while the red curves represents nonresponders who did not demonstrate improvement with the addition of RII12. Notice the increased presence of blue lines curving downward in the female population, indicating cancer cell regression. Notice also the lower average initial cancer cell populations in the female population than the male population.

## 4.4 Discussion

Systems biology methods provide a safe and effective avenue for exploring the potential mechanisms that drive or inhibit favorable patient response to cancer treatments, including targeted immunotherapies. While a mathematical framework may not manage to fully capture the intricacies of the human immune system, its representation of the major immune

processes and interactions between several cell subtypes and signaling molecules allows for discrete analysis of a treatment’s effects, and the identification of macroscopic parameter ranges that are most conducive to treatment response. With this knowledge, it may be possible to recommend a patient-specific therapy and to parameterize a model by examining an individual patient’s specific tumor-immune microenvironment, e.g. via tumor biopsy, to ultimately optimize individual patient treatment protocols.

With the help of experimental calibration and literature-based data, systems biology models can populate a significant patient cohort for large-scale analysis of specific patient subgroups. This study focused on examining the effect of sex-specific immune differences on the response to nivolumab, an anti-PD1 immune checkpoint inhibitor. Thus, large populations reflecting male and female HNSCC patients were generated in order to produce meaningful insight on the difference in treatment response between the sexes and the origin of these differences. Such insight may prove useful for improving treatment outcome for all patients, and particularly for females, who tend to exhibit a lower response rate to cancer immunotherapy [82], [83].

In this work, a thorough literature review was conducted to better understand the differences in the immune system between male and female patients and to recapitulate these differences in the systems biology model. Contextually-relevant parameters were then subjected to a sensitivity analysis to identify a subset of nine parameters  $\Omega$  that ultimately served to differentiate between male and female patients during the generation of virtual populations. Due to limited data in the literature that could be used to quantify the distinct ranges of individual kinetic parameters that are appropriate for male and female patients, we took the nominal ranges that were previously reported [57] to represent the sampling ranges for male virtual patients. We then updated the sampling ranges of the sex-specific parameters  $\Omega$  as appropriate to generate representative female virtual patients that led to sex-specific differences in the immune cell populations that are consistent with those reported in the literature. In simulations of nivolumab treatment, female virtual patient populations were consistently less responsive to treatment than the male population, with the response rates decreasing as parameter sampling ranges were adjusted in the direction of “female” extremes. This suggests that, as consistent with the literature, female patients exhibit lower response to nivolumab than their male counterparts. Indeed, certain sex-specific characteristics described in Table 4.1 may reasonably lead to decreased response rate when placed within the context of the network in Figure 4.1. For instance, higher PD-L1 and PD-1 expression in females leads to increased effects of the PD-L:PD-L1 complex, providing increased inhibition of T-cell activities. Furthermore, decreased CD8+ T-cell differentiation combined with a lower basal fraction of CD8+ naive T-cells (which is further exacerbated by increased CD4+ T-cell proliferation) negatively impacts cytotoxic

functions that help kill cancer cells. Patients who do not respond to nivolumab monotherapy may benefit from combination therapy with, e.g. recombinant IL12, with the latter administered prior to nivolumab to boost the overall response to treatment. During this analysis, one large male population and one large female patient population were generated to examine the sex-specific differences in response to the combination therapy, where the female population was generated by sampling from more extreme parameter ranges than for the nivolumab monotherapy. This enabled the consideration of a high degree of patient variability in the tumor-immune microenvironment. Subjecting both populations to several simulated treatment scenarios comprised of a 10 pg/mL dose of RIL12 given at a specific time (ranging between 0 and 24 hours) prior to nivolumab treatment revealed an apparent larger benefit for female non-responders than male non-responders, with a much higher percentage of females converted into responders due to RIL12. These results may provide rationale for future research, perhaps in a clinical setting, into the combination of RIL12 with nivolumab in patients who do not respond to nivolumab alone. However, given the extremity of the female virtual patient population parameters and the limited literature information available, it remains to be tested whether female patients receive higher benefit from RIL12 pre-treatment than male patients. Nevertheless, in simulations, both sexes exhibited more favourable treatment outcomes when the RIL12 was dosed further in advance of the start of the nivolumab treatment schedule.

Interestingly, when simulating an RIL12 dose of 0 pg/mL, which effectively serves to delay nivolumab treatment in the ex vivo setting, similar trends were observed in simulations; particularly, a few patients of each sex appeared to experience a benefit from a delay in treatment. These counterintuitive results may have arisen due to time related changes in particular parameters which somehow naturally managed to provide a defense against a higher cancer cell count after several hours of growth. Further analysis is required to understand this phenomenon, involving the scrutinizing of the time evolutions of every immune cell population involved in the model. With slightly more female patients experiencing a positive effect from delay than men, the results of the 10 pg/mL RIL12 may be inflated due to the suggested notion that the natural immune processes affecting cell counts and protein concentrations over time before introducing pharmaceutical intervention may serve to better the treatment outcome. This inflation is minimal, however, as only a select few patients out of 100 of each sex experienced a benefit from delayed nivolumab treatment.

While some interesting results have arisen in this study, it is important to note that there are several limitations to the work. For example, the lack of quantitative data that was available in the literature to accurately parameterize sex-specific differences in the model parameters meant that we had to change the parameters by trial-and-error and look at their downstream effect on the immune landscape and response to treatment. Given

that the model may be non-identifiable, it is possible that several distinct parameter sets can lead to similar response to treatment; and it is not straightforward to definitively state whether the sampling ranges used for female patients are in a biologically-relevant range. As such, the results comparing response to both the nivolumab treatment schedule as well as the combination therapy with recombinant IL12 may be misleading. This issue may partially be overcome by the collection and analysis of tumor biopsies for a larger cohort of male and female patients, under both control and treatment conditions. On that note, it is important to point out that the data that was collected to parameterize the sampling ranges for the male patient populations consisted of tumor biopsies from just 50 HNSCC patients. Therefore, the variability in the measured data may not be reflective of the total degree of variability in the tumor-immune microenvironment exhibited by patients. Finally, to remain tractable, several simplifications were made in the mathematical model, such as assumptions that PD-1 and PD-L1 are expressed uniformly across all T-cell populations and that all proteins achieve steady state values instantly. Therefore, the mathematical model does not capture the full complexities of the immune processes and immuno-modulatory effects of treatment. Further expansion of the model to an *in vivo* setting, which includes drug distribution and pharmacokinetics would be warranted before any clinical decisions are made based on the results of the simulations.

As demonstrated by this study, systems biology approaches are generalizable to other contexts and can be used to provide valuable insights into the immunomodulatory effects of a variety of treatments, and for other patient populations. For example, future studies can be performed in a similar fashion to increase the understanding of nivolumab's efficacy among patients of different age groups, perhaps taking into account additional underlying immune conditions that may affect the response to treatment. Moreover, the results of this work have paved a path to better understand the immune characteristics associated with female patients' apparent resistance to treatment when compared to males, which may inform the advent of targeted combination treatments and/or alternative treatment schedules that can help increase treatment efficacy for females. Additionally, the results of the recombinant IL12 simulations provide rationale for future clinical investigations into the impact of timing during combination treatment administration. While this analysis focused strictly on the efficacy of the treatment in treating cancer cells, future endeavors may analyze other model components such as cytokines and T-cell counts to gauge any information regarding the safety of these treatments; while the tumor may be eradicated, patients may experience dangerous side effects due to cytokine population imbalances and other issues. It would thus be a fruitful examination to look at any particularly risk-inducing parameter values after the simulation of treatment in order to inform therapeutic methods that can boast both efficacy and safety.

# Chapter 5

## Conclusion

### 5.1 Summary

Through this thesis, we examined the application of a systems biology model in the study of sex differences in patient response to the anti-PD-1 immune checkpoint inhibitor nivolumab. Indeed, due to known sex imbalances regarding participation in clinical trials, it is important to understand why certain treatments may affect a certain sex differently and what steps may be taken in the future to alleviate any inequalities. Following the discussion of relevant information regarding cancer biology and systems biology, a detailed description of model equations and parameters provided the context needed in order to understand the mechanisms by which the model in question functioned within the study. Specifically, this model was used in conjunction with immune sex differences reported in the literature to generate several sex-specific patient populations. These populations were then subjected to a three-day nivolumab treatment schedule and those who did not respond were further subjected to simulated combination therapy where a dose of recombinant IL12 was given up to 24 hours prior to the same three day nivolumab treatment schedule. Interesting results suggesting differences between male and female response to both of these treatment options arose.

Analysis of over 30 different patient populations representing several variations of female immune systems indicated a distinct male bias in regards to response to nivolumab, appearing to indicate that male patients have a higher chance at responding to the treatment in comparison to their female counterparts. These results appear to echo sentiments drawn from clinical studies [82] that males tend to experience better therapeutic outcomes following administration of several types of immunotherapy. With little to no sex-related

analysis in the literature of patient response to combination therapy with recombinant IL12, results regarding this treatment plan used exaggerated female immune characteristics to compare the rate at which nonresponders to nivolumab alone were able to respond to the additional dosage of recombinant IL12. Conservative conclusions from the comparison between male and female patient populations in this regard to the combination therapy indicate increased benefit for female patients than male. Further examination on particular model parameters influencing these differences is necessary to increase understanding of the dynamics behind sex-influenced treatment response. Indeed, several limitations impacted the study; lack of quantitative data appropriate for the model hindered the accuracy of our representations of the immune profile of each sex. Additionally, the biological dynamics within the immune system and tumor microenvironment are far more complicated than may be represented mathematically. Nevertheless, these results may be useful in future work to develop a more diverse array of treatment options allowing for personalized treatment options and thus better outcomes for all kinds of patients.

## 5.2 Future directions

The complexity and diversity within the immune system allows for all sorts of treatment options employing various cell types in various therapeutic approaches. As such, the possibilities are endless for the usage of systems biology methods in further understanding these treatments and aiding in the development of new strategies to increase efficacy in our fight against cancer. Here, we will introduce a particularly fascinating direction in which systems biology methods much like the ones used in Chapter 4 relating to CAR T-cell therapy. As described in Section 1.4.2, CAR T-cell therapy involves endogenous T-cells that were extracted and engineered with chimeric antigen receptors (CARs) to target particular antigens present on tumor cells and then administered into the body to fight the cancer. In recent years, studies have begun to focus on particular subtypes of T-cell populations, such as CD4+ and CD8+ T-cells, being fitted with CARs and the therapeutic ramifications of each subtype. One potential ramification worth looking into is cytokine release syndrome (CRS), an unfortunate side effect of CAR T-cell therapy during which inflammatory cytokine populations become unbalanced, resulting in uncontrolled inflammatory responses in patients leading to illness and potential death. Naturally, such a side effect is undesirable in the effort to cure one's cancer, so research must be done to devise safer CAR T-cell treatment options while maintaining efficacy. We present a pathway below indicating interactions between CAR T-cells, endogenous immune cells, cancer cells, and key inflammatory cytokines, with CAR T-cells divided into CAR4 (CAR CD4+) and

CAR8 (CAR CD8+) T-cells.

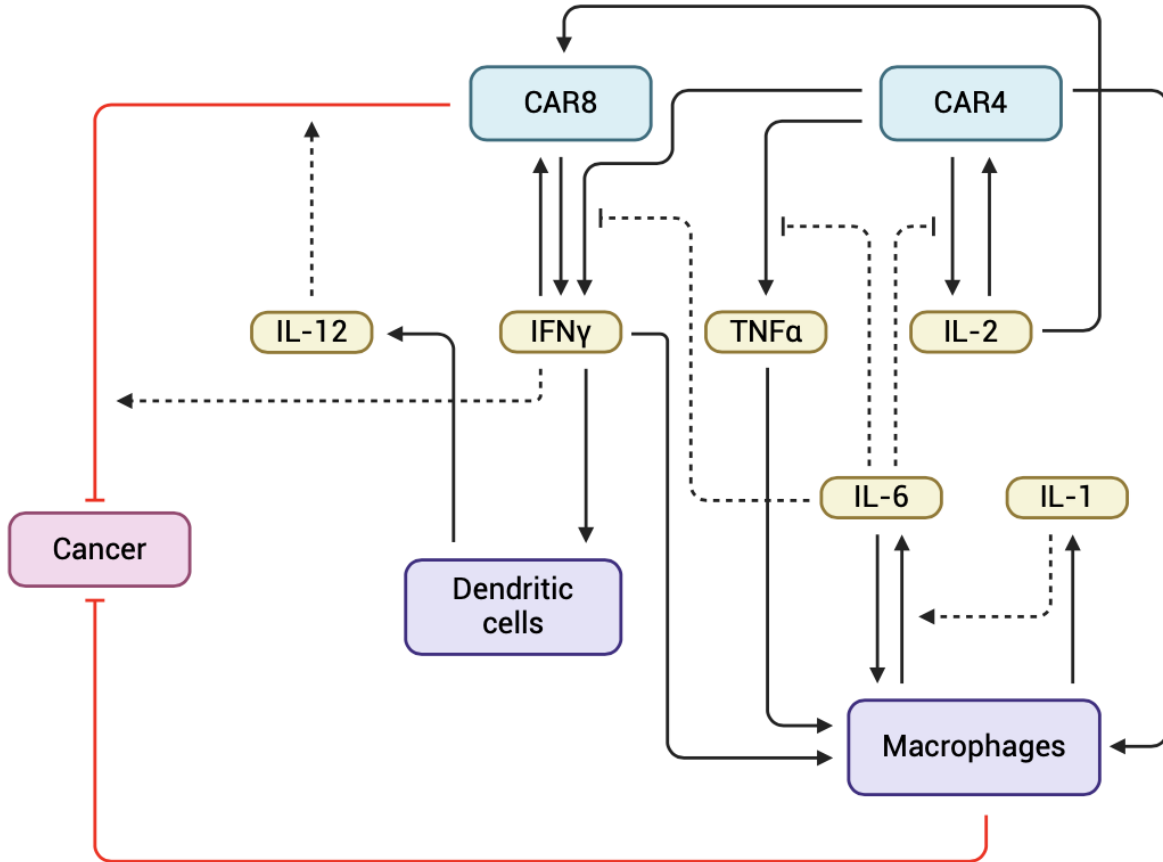


Figure 5.1: Network illustrating interactions between CAR8 and CAR4 cells (blue), key inflammatory cytokines (yellow), endogenous immune cells (purple), and cancer cells (red). Pointed arrowheads indicate upregulation while flat arrowheads indicate inhibition.

By representing the interactions illustrated in Figure 5.1, differential equations can be used to form a mathematical model capable of simulating various CAR T-cell treatment protocols, including experimenting with different CAR4:CAR8 ratios. Results of such simulations can reveal potential risks and benefits associated with different therapeutic plans, offering insight into how this treatment may be developed and administered to patients offering similar or increased anti-tumor activity while reducing the risk of CRS. These insights may also be valuable towards developing personalized therapy. The availability of

in-silico experimentation in this case is particularly valuable as it provides the opportunity for the meaningful data to be collected to inform future drug development without the physical risks associated with in-vivo clinical trials.

# References

- [1] R. H. Wilkins, “Neurosurgical classics—xxiv,” *Journal of Neurosurgery*, vol. 21, no. 10, pp. 892–905, 1964.
- [2] S. I. Hajdu, “A note from history: Landmarks in history of cancer, part 1,” *Cancer*, vol. 117, no. 5, pp. 1097–1102, 2011.
- [3] H. Nagai and Y. H. Kim, “Cancer prevention from the perspective of global cancer burden patterns,” *Journal of thoracic disease*, vol. 9, no. 3, p. 448, 2017.
- [4] A. Di Lonardo, S. Nasi, and S. Pulciani, “Cancer: We should not forget the past,” *Journal of cancer*, vol. 6, no. 1, p. 29, 2015.
- [5] C. Yapijakis, “Hippocrates of kos, the father of clinical medicine, and asclepiades of bithynia, the father of molecular medicine,” *in vivo*, vol. 23, no. 4, pp. 507–514, 2009.
- [6] I. Mitrus, E. Bryndza, A. Sochanik, and S. Szala, “Evolving models of tumor origin and progression,” *Tumor Biology*, vol. 33, pp. 911–917, 2012.
- [7] M. Arruebo, N. Vilaboa, B. Sáez-Gutierrez, *et al.*, “Assessment of the evolution of cancer treatment therapies,” *Cancers*, vol. 3, no. 3, pp. 3279–3330, 2011.
- [8] D. Brenner, A. Poirier, L. Smith, L. Aziz, L. Ellison, N. Fitzgerald, *et al.*, “Canadian cancer statistics advisory committee in collaboration with the canadian cancer society, statistics canada and the public health agency of canada,” *Canadian Cancer Statistics*, vol. 2021, pp. 1–95, 2021.
- [9] G. M. Cooper and K. Adams, *The cell: a molecular approach*. Oxford University Press, 2022.
- [10] B. Alberts, A. Johnson, J. Lewis, M. Raff, K. Roberts, and P. Walter, *Molecular Biology of the Cell. 4th edition*. Garland Science, 2002.
- [11] A. Ashworth, C. J. Lord, and J. S. Reis-Filho, “Genetic interactions in cancer progression and treatment,” *Cell*, vol. 145, no. 1, pp. 30–38, 2011.

- [12] W. Du and J. S. Searle, "The rb pathway and cancer therapeutics," *Current drug targets*, vol. 10, no. 7, pp. 581–589, 2009.
- [13] P. Deininger, "Genetic instability in cancer: Caretaker and gatekeeper genes," *Ochsner Journal*, vol. 1, no. 4, pp. 206–209, 1999.
- [14] J. Shortt and R. W. Johnstone, "Oncogenes in cell survival and cell death," *Cold Spring Harbor perspectives in biology*, vol. 4, no. 12, a009829, 2012.
- [15] B. Pucci, M. Kastan, and A. Giordano, "Cell cycle and apoptosis," *Neoplasia*, vol. 2, no. 4, pp. 291–299, 2000.
- [16] L. Pray, "Dna replication and causes of mutation," *Nature education*, vol. 1, no. 1, p. 214, 2008.
- [17] R. Weinberg, D. Hanahan, *et al.*, "The hallmarks of cancer," *Cell*, vol. 100, no. 1, pp. 57–70, 2000.
- [18] D. Hanahan and R. A. Weinberg, "Hallmarks of cancer: The next generation," *cell*, vol. 144, no. 5, pp. 646–674, 2011.
- [19] J. Fares, M. Y. Fares, H. H. Khachfe, H. A. Salhab, and Y. Fares, "Molecular principles of metastasis: A hallmark of cancer revisited," *Signal transduction and targeted therapy*, vol. 5, no. 1, p. 28, 2020.
- [20] Y. Shiravand, F. Khodadadi, S. M. A. Kashani, *et al.*, "Immune checkpoint inhibitors in cancer therapy," *Current Oncology*, vol. 29, no. 5, pp. 3044–3060, 2022.
- [21] I. Dagogo-Jack and A. T. Shaw, "Tumour heterogeneity and resistance to cancer therapies," *Nature reviews Clinical oncology*, vol. 15, no. 2, pp. 81–94, 2018.
- [22] M. Greaves and C. C. Maley, "Clonal evolution in cancer," *Nature*, vol. 481, no. 7381, pp. 306–313, 2012.
- [23] S. Kelderman, T. N. Schumacher, and J. B. Haanen, "Acquired and intrinsic resistance in cancer immunotherapy," *Molecular oncology*, vol. 8, no. 6, pp. 1132–1139, 2014.
- [24] D. M. Pardoll, "The blockade of immune checkpoints in cancer immunotherapy," *Nature reviews cancer*, vol. 12, no. 4, pp. 252–264, 2012.
- [25] D. T. Debela, S. G. Muzazu, K. D. Heraro, *et al.*, "New approaches and procedures for cancer treatment: Current perspectives," *SAGE open medicine*, vol. 9, p. 20503121211034366, 2021.
- [26] P. Dobosz and T. Dzieciatkowski, "The intriguing history of cancer immunotherapy," *Frontiers in immunology*, vol. 10, p. 496087, 2019.

- [27] Y. Zhang and Z. Zhang, “The history and advances in cancer immunotherapy: Understanding the characteristics of tumor-infiltrating immune cells and their therapeutic implications,” *Cellular & molecular immunology*, vol. 17, no. 8, pp. 807–821, 2020.
- [28] M. Y. Balkhi, *Basics of Chimeric Antigen Receptor (CAR) Immunotherapy*. Academic Press, 2019.
- [29] A. Trewavas, “A brief history of systems biology: “every object that biology studies is a system of systems.” francois jacob (1974).,” *The Plant Cell*, vol. 18, no. 10, pp. 2420–2430, 2006.
- [30] A. Spivey, “Systems biology: The big picture,” *Environmental health perspectives*, vol. 112, no. 16, A938–A943, 2004.
- [31] M. D. Mesarović, “Systems theory and biology—view of a theoretician,” in *Systems Theory and Biology: Proceedings of the III Systems Symposium at Case Institute of Technology*, Springer, 1968, pp. 59–87.
- [32] A. Ma’ayan, “Introduction to network analysis in systems biology,” *Science signaling*, vol. 4, no. 190, tr5–tr5, 2011.
- [33] M. Koutrouli, E. Karatzas, D. Paez-Espino, and G. A. Pavlopoulos, “A guide to conquer the biological network era using graph theory,” *Frontiers in bioengineering and biotechnology*, vol. 8, p. 34, 2020.
- [34] A. Angarita-Rodríguez, Y. González-Giraldo, J. J. Rubio-Mesa, A. F. Aristizábal, A. Pinzón, and J. González, “Control theory and systems biology: Potential applications in neurodegeneration and search for therapeutic targets,” *International Journal of Molecular Sciences*, vol. 25, no. 1, p. 365, 2023.
- [35] C. Cosentino and D. Bates, *Feedback control in systems biology*. Crc Press, 2011.
- [36] S. L. Harris and A. J. Levine, “The p53 pathway: Positive and negative feedback loops,” *Oncogene*, vol. 24, no. 17, pp. 2899–2908, 2005.
- [37] J. Walpole, J. A. Papin, and S. M. Peirce, “Multiscale computational models of complex biological systems,” *Annual review of biomedical engineering*, vol. 15, pp. 137–154, 2013.
- [38] L. V. Schaffer and T. Ideker, “Mapping the multiscale structure of biological systems,” *Cell systems*, vol. 12, no. 6, pp. 622–635, 2021.
- [39] B. P. Ingalls, *Mathematical modeling in systems biology: an introduction*. MIT press, 2013.

- [40] W. Lasek, R. Zagożdżon, and M. Jakobisiak, “Interleukin 12: Still a promising candidate for tumor immunotherapy?” *Cancer Immunology, Immunotherapy*, vol. 63, no. 5, pp. 419–435, 2014.
- [41] S. Sakaguchi, “Regulatory t cells: Key controllers of immunologic self-tolerance,” *Cell*, vol. 101, no. 5, pp. 455–458, 2000.
- [42] J. P. Ridge, F. Di Rosa, and P. Matzinger, “A conditioned dendritic cell can be a temporal bridge between a cd4+ t-helper and a t-killer cell,” *Nature*, vol. 393, no. 6684, p. 474, 1998.
- [43] T. Székely Jr and K. Burrage, “Stochastic simulation in systems biology,” *Computational and structural biotechnology journal*, vol. 12, no. 20-21, pp. 14–25, 2014.
- [44] J. Pleyer and C. Fleck, “Agent-based models in cellular systems,” *Frontiers in Physics*, vol. 10, p. 968409, 2023.
- [45] C. M. Micheel, S. J. Nass, G. S. Omenn, *et al.*, “Omics-based clinical discovery: Science, technology, and applications,” in *Evolution of Translational Omics: Lessons Learned and the Path Forward*, National Academies Press (US), 2012.
- [46] B. Karahalil, “Overview of systems biology and omics technologies,” *Current medicinal chemistry*, vol. 23, no. 37, pp. 4221–4230, 2016.
- [47] V. Gligorijević and N. Pržulj, “Methods for biological data integration: Perspectives and challenges,” *Journal of the Royal Society Interface*, vol. 12, no. 112, p. 20150571, 2015.
- [48] A. Özen, M. Gönen, E. Alpaydın, and T. Haliloğlu, “Machine learning integration for predicting the effect of single amino acid substitutions on protein stability,” *BMC Structural Biology*, vol. 9, pp. 1–17, 2009.
- [49] R. Braun, “Systems analysis of high-throughput data,” *A Systems Biology Approach to Blood*, pp. 153–187, 2014.
- [50] B. B. Garana, J. H. Joly, A. Delfarah, H. Hong, and N. A. Graham, “Drug mechanism enrichment analysis improves prioritization of therapeutics for repurposing,” *BMC bioinformatics*, vol. 24, no. 1, p. 215, 2023.
- [51] M. Ashburner, C. A. Ball, J. A. Blake, *et al.*, “Gene ontology: Tool for the unification of biology,” *Nature genetics*, vol. 25, no. 1, pp. 25–29, 2000.
- [52] K. A. Rejniak, *Systems Biology of Tumor Microenvironment: Quantitative Modeling and Simulations*. Springer, 2016, vol. 936.

- [53] D. GuhaThakurta, N. A. Sheikh, T. C. Meagher, S. Letarte, and J. B. Trager, “Applications of systems biology in cancer immunotherapy: From target discovery to biomarkers of clinical outcome,” *Expert Review of Clinical Pharmacology*, vol. 6, no. 4, pp. 387–401, 2013.
- [54] F. V. Filipp, “Precision medicine driven by cancer systems biology,” *Cancer and Metastasis Reviews*, vol. 36, pp. 91–108, 2017.
- [55] B. de Jesus Rodrigues, L. R. C. Barros, and R. C. Almeida, “Three-compartment model of car t-cell immunotherapy,” *bioRxiv*, p. 779793, 2019.
- [56] M. Smalley, M. Przedborski, S. Thiyagarajan, *et al.*, “Integrating systems biology and an ex vivo human tumor model elucidates pd-1 blockade response dynamics,” *Iscience*, vol. 23, no. 6, 2020.
- [57] M. Przedborski, M. Smalley, S. Thiyagarajan, A. Goldman, and M. Kohandel, “Systems biology informed neural networks (sbinn) predict response and novel combinations for pd-1 checkpoint blockade,” *Communications Biology*, vol. 4, no. 877, 2021. DOI: [10.1038/s42003-021-02393-7](https://doi.org/10.1038/s42003-021-02393-7).
- [58] A. Yates, C. Bergmann, J. L. Van Hemmen, J. Stark, and R. Callard, “Cytokine-modulated regulation of helper t cell populations,” *Journal of theoretical biology*, vol. 206, no. 4, pp. 539–560, 2000.
- [59] S. Diehl and M. Rincón, “The two faces of il-6 on th1/th2 differentiation,” *Molecular immunology*, vol. 39, no. 9, pp. 531–536, 2002.
- [60] G. J. Freeman, E. J. Wherry, R. Ahmed, and A. H. Sharpe, “Reinvigorating exhausted hiv-specific t cells via pd-1–pd-1 ligand blockade,” *Journal of Experimental Medicine*, vol. 203, no. 10, pp. 2223–2227, 2006.
- [61] T. Okazaki and T. Honjo, “The pd-1–pd-1 pathway in immunological tolerance,” *Trends in immunology*, vol. 27, no. 4, pp. 195–201, 2006.
- [62] M. Sznol and L. Chen, “Antagonist antibodies to pd-1 and b7-h1 (pd-l1) in the treatment of advanced human cancer—response,” *Clinical Cancer Research*, vol. 19, no. 19, pp. 5542–5542, 2013.
- [63] M. A. Fishman and A. S. Perelson, “Th1/th2 cross regulation,” *Journal of theoretical biology*, vol. 170, no. 1, pp. 25–56, 1994.
- [64] J. A. Trapani and M. J. Smyth, “Functional significance of the perforin/granzyme cell death pathway,” *Nature Reviews Immunology*, vol. 2, no. 10, p. 735, 2002.
- [65] M. A. Fishman and A. S. Perelson, “Th1/th2 differentiation and cross-regulation,” *Bulletin of mathematical biology*, vol. 61, no. 3, pp. 403–436, 1999.

- [66] S. Romagnani, “The th1/th2 paradigm,” *Immunology today*, vol. 18, no. 6, pp. 263–266, 1997.
- [67] M. Rincón, J. Anguita, T. Nakamura, E. Fikrig, and R. A. Flavell, “Interleukin (il)-6 directs the differentiation of il-4-producing cd4+ t cells,” *Journal of Experimental Medicine*, vol. 185, no. 3, pp. 461–470, 1997.
- [68] S. E. Macatonia, N. A. Hosken, M. Litton, *et al.*, “Dendritic cells produce il-12 and direct the development of th1 cells from naive cd4+ t cells,” *The Journal of Immunology*, vol. 154, no. 10, pp. 5071–5079, 1995.
- [69] V. Carreño, S. Zeuzem, U. Hopf, *et al.*, “A phase i/ii study of recombinant human interleukin-12 in patients with chronic hepatitis b,” *Journal of hepatology*, vol. 32, no. 2, pp. 317–324, 2000.
- [70] B. F. Morel, J. Kalagnanam, and P. A. Morel, “Mathematical modeling of th1-th2 dynamics,” in *Theoretical and experimental insights into immunology*, Springer, 1992, pp. 171–190.
- [71] X. Lai and A. Friedman, “Combination therapy of cancer with cancer vaccine and immune checkpoint inhibitors: A mathematical model,” *PLoS One*, vol. 12, no. 5, e0178479, 2017.
- [72] D. C. DeLucia and J. K. Lee, “Development of cancer immunotherapies,” *Cancer treatment and research*, vol. 183, pp. 1–48, 2022. DOI: [10.1007/978-3-030-96376-7\\_1](https://doi.org/10.1007/978-3-030-96376-7_1).
- [73] E. B. Garon, *Cancer immunotherapy trials not immune from imprecise selection of patients*, 2017.
- [74] H. Zhang and J. Chen, “Current status and future directions of cancer immunotherapy,” *Journal of cancer*, vol. 9, no. 10, p. 1773, 2018.
- [75] M. Guha, “The new era of immune checkpoint inhibitors,” *Acute pain*, vol. 10, p. 00, 2019.
- [76] B. C. Özdemir and G.-P. Dotto, “Sex hormones and anticancer immunity,” *Clinical Cancer Research*, vol. 25, no. 15, pp. 4603–4610, 2019.
- [77] G. Neigh and M. Mitzelfelt, *Sex differences in physiology*. Academic Press, 2016.
- [78] P. Giovannelli, M. Di Donato, G. Galasso, *et al.*, “Breast cancer stem cells: The role of sex steroid receptors,” *World Journal of Stem Cells*, vol. 11, no. 9, p. 594, 2019.
- [79] X.-D. Fu, E. Russo, S. Zullino, A. R. Genazzani, and T. Simoncini, “Sex steroids and breast cancer metastasis,” *Hormone Molecular Biology and Clinical Investigation*, vol. 3, no. 2, pp. 383–389, 2010.

- [80] P. Christoforou, P. F. Christopoulos, and M. Koutsilieris, “The role of estrogen receptor  $\beta$  in prostate cancer,” *Molecular medicine*, vol. 20, pp. 427–434, 2014.
- [81] V. Taneja, “Sex hormones determine immune response,” *Frontiers in immunology*, vol. 9, p. 386 034, 2018.
- [82] F. Conforti, L. Pala, V. Bagnardi, *et al.*, “Cancer immunotherapy efficacy and patients’ sex: A systematic review and meta-analysis,” *The Lancet Oncology*, vol. 19, no. 6, pp. 737–746, 2018.
- [83] S. Wang, L. A. Cowley, and X.-S. Liu, “Sex differences in cancer immunotherapy efficacy, biomarkers, and therapeutic strategy,” *Molecules*, vol. 24, no. 18, p. 3214, 2019.
- [84] S. L. Klein and K. L. Flanagan, “Sex differences in immune responses,” *Nature Reviews Immunology*, vol. 16, no. 10, pp. 626–638, 2016.
- [85] K. A. Liu and N. A. Dipietro Mager, “Women’s involvement in clinical trials: Historical perspective and future implications,” *Pharmacy Practice (Granada)*, vol. 14, no. 1, pp. 0–0, 2016.
- [86] I. Capone, P. M. P. A. Ascierio, W. Malorni, and L. Gabriele, “Sexual dimorphism of immune responses: A new perspective in cancer immunotherapy,” *Frontiers in Immunology*, 2018. DOI: [10.3389/fimmu.2018.00552](https://doi.org/10.3389/fimmu.2018.00552).
- [87] M. A. Zhang, D. Rego, M. Moshkova, *et al.*, “Preoxisome proliferator-activated receptor ( $\text{ppar}$ ) $\alpha$  and  $-\gamma$  regulate  $\text{ifn}\gamma$  and  $\text{il-17a}$  production by human t cells in a sex-specific way,” *Proc Natl Acad Sci U S A*, vol. 9, 2012. DOI: [10.1073/pnas.1118458109](https://doi.org/10.1073/pnas.1118458109).
- [88] Y. Gu, Y. Y. Tang, J. X. Wa, *et al.*, “Sex difference in the expression of pd-1 of non-small cell lung cancer,” *Frontiers in Immunology*, 2022. DOI: [10.3389/fimmu.2022.1026214](https://doi.org/10.3389/fimmu.2022.1026214).
- [89] Y.-M. Lin, W.-W. Sung, M.-J. Hsieh, *et al.*, “High pd-1 expression correlates with metastasis and poor prognosis in oral squamous cell carcinoma,” *PLoS One*, 2015. DOI: [10.1371/journal.pone.0142656](https://doi.org/10.1371/journal.pone.0142656).
- [90] T. Hussain, A. Kallies, and A. Vasanthakumar, “Sex-bias in  $\text{cd8}+$  t-cell stemness and exhaustion in cancer,” *Clinical and Translational immunology*, vol. 11, 2022. DOI: [10.1002/cti2.1414](https://doi.org/10.1002/cti2.1414).

- [91] F. Formiga, A. Ferrer, G. Padros, A. L. Soto, M. Sarro, and R. Pujol, “Differences according to gender and health status in cd4: Cd8 ratio in a sample of community-dwelling oldest old. the octabaix immune study,” *Aging Clinical and Experimental Research*, vol. 23, pp. 268–272, 2011.
- [92] T. M. Inc., *Rand*, Natick, Massachusetts, United States, 2024. [Online]. Available: <https://www.mathworks.com/help/matlab/ref/rand.html>.
- [93] J. R. McIntosh, “Mitosis,” *Cold Spring Harbor perspectives in biology*, vol. 8, no. 9, a023218, 2016.
- [94] I. F. Tannock, J. A. Hickman, *et al.*, “Limits to personalized cancer medicine,” *N Engl J Med*, vol. 375, no. 13, pp. 1289–1294, 2016.
- [95] B. Majumder, U. Baraneedharan, S. Thiyagarajan, *et al.*, “Predicting clinical response to anticancer drugs using an ex vivo platform that captures tumour heterogeneity,” *Nature communications*, vol. 6, no. 1, pp. 1–14, 2015.
- [96] Z. Zi, “Sensitivity analysis approaches applied to systems biology models,” *IET systems biology*, vol. 5, no. 6, pp. 336–346, 2011.
- [97] G. M. Hornberger and R. C. Spear, “Approach to the preliminary analysis of environmental systems,” *J. Environ. Mgmt.*, vol. 12, no. 1, pp. 7–18, 1981.
- [98] K.-H. Cho, S.-Y. Shin, W. Kolch, and O. Wolkenhauer, “Experimental design in systems biology, based on parameter sensitivity analysis using a monte carlo method: A case study for the tnfa-mediated nf- $\kappa$  b signal transduction pathway,” *Simulation*, vol. 79, no. 12, pp. 726–739, 2003.
- [99] Z. Zi, K.-H. Cho, M.-H. Sung, X. Xia, J. Zheng, and Z. Sun, “In silico identification of the key components and steps in ifn- $\gamma$  induced jak-stat signaling pathway,” *FEBS letters*, vol. 579, no. 5, pp. 1101–1108, 2005.
- [100] S. Haykin, *Neural Networks and Learning Machines, 3/E*. Pearson Education India, 2010.
- [101] C. M. Bishop, *Pattern recognition and machine learning*. springer, 2006.
- [102] S. J. Pan and Q. Yang, “A survey on transfer learning,” *IEEE Transactions on knowledge and data engineering*, vol. 22, no. 10, pp. 1345–1359, 2009.
- [103] S. Lloyd, “Least squares quantization in pcm,” *IEEE transactions on information theory*, vol. 28, no. 2, pp. 129–137, 1982.
- [104] M. D. McKay, R. J. Beckman, and W. J. Conover, “Comparison of three methods for selecting values of input variables in the analysis of output from a computer code,” *Technometrics*, vol. 21, no. 2, pp. 239–245, 1979.

- [105] A. Tharwat, T. Gaber, A. Ibrahim, and A. E. Hassanien, “Linear discriminant analysis: A detailed tutorial,” *AI communications*, vol. 30, no. 2, pp. 169–190, 2017.
- [106] W. Krzanowski, *Principles of multivariate analysis*. OUP Oxford, 2000, vol. 23.
- [107] I. T. Jolliffe, “Graphical representation of data using principal components,” *Principal component analysis*, pp. 78–110, 2002.
- [108] R. Kohavi, G. H. John, *et al.*, “Wrappers for feature subset selection,” *Artificial intelligence*, vol. 97, no. 1-2, pp. 273–324, 1997.
- [109] I. The MathWorks. “Selecting features for classifying high-dimensional data.” (), [Online]. Available: <https://www.mathworks.com/help/stats/examples/selecting-features-for-classifying-high-dimensional-data.html> (visited on 2020).
- [110] K. M. Redmond, T. R. Wilson, P. G. Johnston, and D. B. Longley, “Resistance mechanisms to cancer chemotherapy,” *Front Biosci*, vol. 13, pp. 5138–5154, 2008.
- [111] A. O. Pisco and S. Huang, “Non-genetic cancer cell plasticity and therapy-induced stemness in tumour relapse: ‘what does not kill me strengthens me’,” *British journal of cancer*, vol. 112, no. 11, pp. 1725–1732, 2015.
- [112] J. M. Bauml, C. Aggarwal, and R. B. Cohen, “Immunotherapy for head and neck cancer: Where are we now and where are we going?” *Annals of Translational Medicine*, vol. 7, no. Suppl 3, 2019.
- [113] L. v. d. Maaten and G. Hinton, “Visualizing data using t-sne,” *Journal of machine learning research*, vol. 9, no. Nov, pp. 2579–2605, 2008.
- [114] D. Castelvechi, “Can we open the black box of ai?” *Nature News*, vol. 538, no. 7623, p. 20, 2016.
- [115] S. E. Geerlings and A. I. Hoepelman, “Immune dysfunction in patients with diabetes mellitus (dm),” *FEMS Immunology & Medical Microbiology*, vol. 26, no. 3-4, pp. 259–265, 1999.
- [116] J. K. Nicholson, “Global systems biology, personalized medicine and molecular epidemiology,” *Molecular systems biology*, vol. 2, no. 1, 2006.
- [117] H.-Y. Chuang, M. Hofree, and T. Ideker, “A decade of systems biology,” *Annual review of cell and developmental biology*, vol. 26, pp. 721–744, 2010.
- [118] J. Loscalzo and A.-L. Barabasi, “Systems biology and the future of medicine,” *Wiley Interdisciplinary Reviews: Systems Biology and Medicine*, vol. 3, no. 6, pp. 619–627, 2011.

- [119] S. Greenblum, P. J. Turnbaugh, and E. Borenstein, “Metagenomic systems biology of the human gut microbiome reveals topological shifts associated with obesity and inflammatory bowel disease,” *Proceedings of the National Academy of Sciences*, vol. 109, no. 2, pp. 594–599, 2012.
- [120] H. A. Ebhardt, A. Root, C. Sander, and R. Aebersold, “Applications of targeted proteomics in systems biology and translational medicine,” *Proteomics*, vol. 15, no. 18, pp. 3193–3208, 2015.
- [121] N. N. Parikhshak, M. J. Gandal, and D. H. Geschwind, “Systems biology and gene networks in neurodevelopmental and neurodegenerative disorders,” *Nature Reviews Genetics*, vol. 16, no. 8, pp. 441–458, 2015.
- [122] J. J. Hornberg, F. J. Bruggeman, H. V. Westerhoff, and J. Lankelma, “Cancer: A systems biology disease,” *Biosystems*, vol. 83, no. 2-3, pp. 81–90, 2006.
- [123] K. M. Mani, C. Lefebvre, K. Wang, *et al.*, “A systems biology approach to prediction of oncogenes and molecular perturbation targets in b-cell lymphomas,” *Molecular systems biology*, vol. 4, no. 1, 2008.
- [124] D. Faratian, A. Goltsov, G. Lebedeva, *et al.*, “Systems biology reveals new strategies for personalizing cancer medicine and confirms the role of pten in resistance to trastuzumab,” *Cancer research*, vol. 69, no. 16, pp. 6713–6720, 2009.
- [125] P. K. Kreeger and D. A. Lauffenburger, “Cancer systems biology: A network modeling perspective,” *Carcinogenesis*, vol. 31, no. 1, pp. 2–8, 2010.
- [126] C. M. Perou and A.-L. Børresen-Dale, “Systems biology and genomics of breast cancer,” *Cold Spring Harbor perspectives in biology*, vol. 3, no. 2, a003293, 2011.
- [127] E. Barillot, L. Calzone, P. Hupe, J.-P. Vert, and A. Zinovyev, *Computational systems biology of cancer*. CRC Press, 2012.
- [128] Y. Yarden and G. Pines, “The erbb network: At last, cancer therapy meets systems biology,” *Nature Reviews Cancer*, vol. 12, no. 8, pp. 553–563, 2012.
- [129] E. Wang, J. Zou, N. Zaman, L. K. Beitel, M. Trifiro, and M. Paliouras, “Cancer systems biology in the genome sequencing era: Part 2, evolutionary dynamics of tumor clonal networks and drug resistance,” in *Seminars in cancer biology*, Elsevier, vol. 23(4), 2013, pp. 286–292.
- [130] L. Galluzzi, I. Vitale, J. Michels, *et al.*, “Systems biology of cisplatin resistance: Past, present and future,” *Cell death & disease*, vol. 5, no. 5, e1257–e1257, 2014.
- [131] E. C. Butcher, E. L. Berg, and E. J. Kunkel, “Systems biology in drug discovery,” *Nature biotechnology*, vol. 22, no. 10, pp. 1253–1259, 2004.

- [132] A. Bugrim, T. Nikolskaya, and Y. Nikolsky, “Early prediction of drug metabolism and toxicity: Systems biology approach and modeling,” *Drug discovery today*, vol. 9, no. 3, pp. 127–135, 2004.
- [133] E. C. Butcher, “Can cell systems biology rescue drug discovery?” *Nature Reviews Drug Discovery*, vol. 4, no. 6, pp. 461–467, 2005.
- [134] E. Berg, E. Kunkel, and E. Hytopoulos, “Biological complexity and drug discovery: A practical systems biology approach,” *IEE Proceedings-Systems Biology*, vol. 152, no. 4, pp. 201–206, 2005.
- [135] O. Keskin, A. Gursoy, B. Ma, and R. Nussinov, “Towards drugs targeting multiple proteins in a systems biology approach,” *Current topics in medicinal chemistry*, vol. 7, no. 10, pp. 943–951, 2007.
- [136] J. Zhu, B. Zhang, and E. E. Schadt, “A systems biology approach to drug discovery,” *Advances in genetics*, vol. 60, pp. 603–635, 2008.
- [137] D. Arrell and A. Terzic, “Network systems biology for drug discovery,” *Clinical Pharmacology & Therapeutics*, vol. 88, no. 1, pp. 120–125, 2010.
- [138] A. Pujol, R. Mosca, J. Farrés, and P. Aloy, “Unveiling the role of network and systems biology in drug discovery,” *Trends in pharmacological sciences*, vol. 31, no. 3, pp. 115–123, 2010.
- [139] A. S. Azmi, Z. Wang, P. A. Philip, R. M. Mohammad, and F. H. Sarkar, “Proof of concept: Network and systems biology approaches aid in the discovery of potent anticancer drug combinations,” *Molecular cancer therapeutics*, vol. 9, no. 12, pp. 3137–3144, 2010.
- [140] R. Burbidge, M. Trotter, B. Buxton, and S. Holden, “Drug design by machine learning: Support vector machines for pharmaceutical data analysis,” *Computers & chemistry*, vol. 26, no. 1, pp. 5–14, 2001.
- [141] S. Agarwal, D. Dugar, and S. Sengupta, “Ranking chemical structures for drug discovery: A new machine learning approach,” *Journal of chemical information and modeling*, vol. 50, no. 5, pp. 716–731, 2010.
- [142] M. P. Menden, F. Iorio, M. Garnett, *et al.*, “Machine learning prediction of cancer cell sensitivity to drugs based on genomic and chemical properties,” *PLoS one*, vol. 8, no. 4, 2013.
- [143] A. Lavecchia, “Machine-learning approaches in drug discovery: Methods and applications,” *Drug discovery today*, vol. 20, no. 3, pp. 318–331, 2015.

- [144] A. N. Lima, E. A. Philot, G. H. G. Trossini, L. P. B. Scott, V. G. Maltarollo, and K. M. Honorio, "Use of machine learning approaches for novel drug discovery," *Expert opinion on drug discovery*, vol. 11, no. 3, pp. 225–239, 2016.
- [145] L. Zhang, J. Tan, D. Han, and H. Zhu, "From machine learning to deep learning: Progress in machine intelligence for rational drug discovery," *Drug discovery today*, vol. 22, no. 11, pp. 1680–1685, 2017.
- [146] Y.-C. Lo, S. E. Rensi, W. Torng, and R. B. Altman, "Machine learning in chemoinformatics and drug discovery," *Drug discovery today*, vol. 23, no. 8, pp. 1538–1546, 2018.
- [147] H. Chen, O. Engkvist, Y. Wang, M. Olivecrona, and T. Blaschke, "The rise of deep learning in drug discovery," *Drug discovery today*, vol. 23, no. 6, pp. 1241–1250, 2018.
- [148] J. Vamathevan, D. Clark, P. Czodrowski, *et al.*, "Applications of machine learning in drug discovery and development," *Nature Reviews Drug Discovery*, vol. 18, no. 6, pp. 463–477, 2019.
- [149] M. Hilario, A. Kalousis, M. Müller, and C. Pellegrini, "Machine learning approaches to lung cancer prediction from mass spectra," *Proteomics*, vol. 3, no. 9, pp. 1716–1719, 2003.
- [150] J. A. Cruz and D. S. Wishart, "Applications of machine learning in cancer prediction and prognosis," *Cancer informatics*, vol. 2, p. 117693510600200030, 2006.
- [151] G. R. Kumar, G. Ramachandra, and K. Nagamani, "An efficient prediction of breast cancer data using data mining techniques," *International Journal of Innovations in Engineering and Technology (IJJET)*, vol. 2, no. 4, p. 139, 2013.
- [152] K. Kourou, T. P. Exarchos, K. P. Exarchos, M. V. Karamouzis, and D. I. Fotiadis, "Machine learning applications in cancer prognosis and prediction," *Computational and structural biotechnology journal*, vol. 13, pp. 8–17, 2015.
- [153] S. Agrawal and J. Agrawal, "Neural network techniques for cancer prediction: A survey," *Procedia Computer Science*, vol. 60, pp. 769–774, 2015.
- [154] M.-W. Huang, C.-W. Chen, W.-C. Lin, S.-W. Ke, and C.-F. Tsai, "Svm and svm ensembles in breast cancer prediction," *PloS one*, vol. 12, no. 1, 2017.
- [155] Y. Xiao, J. Wu, Z. Lin, and X. Zhao, "A deep learning-based multi-model ensemble method for cancer prediction," *Computer methods and programs in biomedicine*, vol. 153, pp. 1–9, 2018.

- [156] T. Kadir and F. Gleeson, “Lung cancer prediction using machine learning and advanced imaging techniques,” *Translational lung cancer research*, vol. 7, no. 3, p. 304, 2018.
- [157] W. H. Wolberg, W. N. Street, and O. L. Mangasarian, “Image analysis and machine learning applied to breast cancer diagnosis and prognosis,” *Analytical and Quantitative cytology and histology*, vol. 17, no. 2, pp. 77–87, 1995.
- [158] K.-B. Hwang, D.-Y. Cho, S.-W. Park, S.-D. Kim, and B.-T. Zhang, “Applying machine learning techniques to analysis of gene expression data: Cancer diagnosis,” in *Methods of microarray data analysis*, Springer, 2002, pp. 167–182.
- [159] K. Polat and S. Güneş, “Breast cancer diagnosis using least square support vector machine,” *Digital signal processing*, vol. 17, no. 4, pp. 694–701, 2007.
- [160] M. F. Akay, “Support vector machines combined with feature selection for breast cancer diagnosis,” *Expert systems with applications*, vol. 36, no. 2, pp. 3240–3247, 2009.
- [161] T. Abeel, T. Helleputte, Y. Van de Peer, P. Dupont, and Y. Saeys, “Robust biomarker identification for cancer diagnosis with ensemble feature selection methods,” *Bioinformatics*, vol. 26, no. 3, pp. 392–398, 2010.
- [162] R. Ramos-Pollán, M. A. Guevara-López, C. Suárez-Ortega, *et al.*, “Discovering mammography-based machine learning classifiers for breast cancer diagnosis,” *Journal of medical systems*, vol. 36, no. 4, pp. 2259–2269, 2012.
- [163] R. Fakoor, F. Ladhak, A. Nazi, and M. Huber, “Using deep learning to enhance cancer diagnosis and classification,” in *Proceedings of the international conference on machine learning*, ACM New York, USA, vol. 28, 2013.
- [164] H. Asri, H. Mousannif, H. Al Moatassime, and T. Noel, “Using machine learning algorithms for breast cancer risk prediction and diagnosis,” *Procedia Computer Science*, vol. 83, pp. 1064–1069, 2016.
- [165] W. Sun, B. Zheng, and W. Qian, “Computer aided lung cancer diagnosis with deep learning algorithms,” in *Medical imaging 2016: computer-aided diagnosis*, International Society for Optics and Photonics, vol. 9785, 2016, 97850Z.
- [166] G. Manogaran, V. Vijayakumar, R. Varatharajan, P. M. Kumar, R. Sundarasekar, and C.-H. Hsu, “Machine learning based big data processing framework for cancer diagnosis using hidden markov model and gm clustering,” *Wireless personal communications*, vol. 102, no. 3, pp. 2099–2116, 2018.

- [167] Z. Liao, D. Li, X. Wang, L. Li, and Q. Zou, “Cancer diagnosis through isomir expression with machine learning method,” *Current Bioinformatics*, vol. 13, no. 1, pp. 57–63, 2018.
- [168] Y. Zhao, M. R. Kosorok, and D. Zeng, “Reinforcement learning design for cancer clinical trials,” *Statistics in medicine*, vol. 28, no. 26, pp. 3294–3315, 2009.
- [169] C. Huang, R. Mezecev, J. F. McDonald, and F. Vannberg, “Open source machine-learning algorithms for the prediction of optimal cancer drug therapies,” *PLoS One*, vol. 12, no. 10, 2017.
- [170] R. Padmanabhan, N. Meskin, and W. M. Haddad, “Reinforcement learning-based control of drug dosing for cancer chemotherapy treatment,” *Mathematical biosciences*, vol. 293, pp. 11–20, 2017.
- [171] M. Komorowski, L. A. Celi, O. Badawi, A. C. Gordon, and A. A. Faisal, “The artificial intelligence clinician learns optimal treatment strategies for sepsis in intensive care,” *Nature medicine*, vol. 24, no. 11, pp. 1716–1720, 2018.
- [172] Y. Wang, H. Fu, and D. Zeng, “Learning optimal personalized treatment rules in consideration of benefit and risk: With an application to treating type 2 diabetes patients with insulin therapies,” *Journal of the American Statistical Association*, vol. 113, no. 521, pp. 1–13, 2018.
- [173] O. Atan, J. Jordon, and M. van der Schaar, “Deep-treat: Learning optimal personalized treatments from observational data using neural networks,” in *Thirty-Second AAAI Conference on Artificial Intelligence*, 2018.
- [174] G. Yauney and P. Shah, “Reinforcement learning with action-derived rewards for chemotherapy and clinical trial dosing regimen selection,” in *Machine Learning for Healthcare Conference*, 2018, pp. 161–226.
- [175] MATLAB, *Release 2018b*. Natick, Massachusetts: The MathWorks Inc., 2018.
- [176] F. Chollet, *Keras*, <https://github.com/fchollet/keras>, 2015.
- [177] Martín Abadi, Ashish Agarwal, Paul Barham, *et al.*, *TensorFlow: Large-scale machine learning on heterogeneous systems*, Software available from tensorflow.org, 2015. [Online]. Available: <https://www.tensorflow.org/>.
- [178] D. P. Kingma and J. Ba, “Adam: A method for stochastic optimization,” *arXiv preprint arXiv:1412.6980*, 2014.
- [179] J. M. Johnson and T. M. Khoshgoftaar, “Survey on deep learning with class imbalance,” *Journal of Big Data*, vol. 6, no. 1, p. 27, 2019.

- [180] F. Pedregosa, G. Varoquaux, A. Gramfort, *et al.*, “Scikit-learn: Machine learning in Python,” *Journal of Machine Learning Research*, vol. 12, pp. 2825–2830, 2011.
- [181] Q. Gu, L. Zhu, and Z. Cai, “Evaluation measures of the classification performance of imbalanced data sets,” in *International symposium on intelligence computation and applications*, Springer, 2009, pp. 461–471.
- [182] J. Cohen, “A coefficient of agreement for nominal scales,” *Educational and psychological measurement*, vol. 20, no. 1, pp. 37–46, 1960.
- [183] I. Witten, E. Frank, M. Hall, and C. Pal, *Data mining fourth edition: Practical machine learning tools and techniques*, 2016.
- [184] B. W. Matthews, “Comparison of the predicted and observed secondary structure of t4 phage lysozyme,” *Biochimica et Biophysica Acta (BBA)-Protein Structure*, vol. 405, no. 2, pp. 442–451, 1975.
- [185] S. Boughorbel, F. Jarray, and M. El-Anbari, “Optimal classifier for imbalanced data using matthews correlation coefficient metric,” *PloS one*, vol. 12, no. 6, 2017.
- [186] C. X. Ling and C. Li, “Data mining for direct marketing: Problems and solutions,” in *Kdd*, vol. 98, 1998, pp. 73–79.
- [187] J. Davis and M. Goadrich, “The relationship between precision-recall and roc curves,” in *Proceedings of the 23rd international conference on Machine learning*, 2006, pp. 233–240.
- [188] M. Goadrich, L. Oliphant, and J. Shavlik, “Gleaner: Creating ensembles of first-order clauses to improve recall-precision curves,” *Machine Learning*, vol. 64, no. 1-3, pp. 231–261, 2006.
- [189] T. Saito and M. Rehmsmeier, “The precision-recall plot is more informative than the roc plot when evaluating binary classifiers on imbalanced datasets,” *PloS one*, vol. 10, no. 3, 2015.
- [190] E. B. Fowlkes and C. L. Mallows, “A method for comparing two hierarchical clusterings,” *Journal of the American statistical association*, vol. 78, no. 383, pp. 553–569, 1983.
- [191] D. D. Lewis and W. A. Gale, “A sequential algorithm for training text classifiers,” in *SIGIR’94*, Springer, 1994, pp. 3–12.
- [192] Q. Zou, S. Xie, Z. Lin, M. Wu, and Y. Ju, “Finding the best classification threshold in imbalanced classification,” *Big Data Research*, vol. 5, pp. 2–8, 2016.

- [193] C. S. Garris, S. P. Arlauckas, R. H. Kohler, *et al.*, “Successful anti-pd-1 cancer immunotherapy requires t cell-dendritic cell crosstalk involving the cytokines ifn- $\gamma$  and il-12,” *Immunity*, vol. 49, no. 6, pp. 1148–1161, 2018.
- [194] H. Tsukamoto, K. Fujieda, A. Miyashita, *et al.*, “Combined blockade of il6 and pd-1/pd-l1 signaling abrogates mutual regulation of their immunosuppressive effects in the tumor microenvironment,” *Cancer research*, vol. 78, no. 17, pp. 5011–5022, 2018.
- [195] S. Sarosiek, R. Shah, and N. C. Munshi, “Review of siltuximab in the treatment of multicentric castlemans disease,” *Therapeutic advances in hematology*, vol. 7, no. 6, pp. 360–366, 2016.
- [196] M. S. Gokhale, V. Vainstein, J. Tom, *et al.*, “Single low-dose rhil-12 safely triggers multilineage hematopoietic and immune-mediated effects,” *Experimental hematology & oncology*, vol. 3, no. 1, p. 11, 2014.
- [197] K. H. Kim, J. Cho, B. M. Ku, *et al.*, “The first-week proliferative response of peripheral blood pd-1+ cd8+ t cells predicts the response to anti-pd-1 therapy in solid tumors,” *Clinical Cancer Research*, vol. 25, no. 7, pp. 2144–2154, 2019.
- [198] K. H. Kim, C. G. Kim, and E.-C. Shin, “Peripheral blood immune cell-based biomarkers in anti-pd-1/pd-l1 therapy,” *Immune Network*, vol. 20, no. 1, 2020.
- [199] K. I. Kim, K. H. Lee, T. R. Kim, Y. S. Chun, T. H. Lee, and H. K. Park, “Ki-67 as a predictor of response to neoadjuvant chemotherapy in breast cancer patients,” *Journal of breast cancer*, vol. 17, no. 1, pp. 40–46, 2014.
- [200] M. P. Pender, “Cd8+ t-cell deficiency, epstein-barr virus infection, vitamin d deficiency, and steps to autoimmunity: A unifying hypothesis,” *Autoimmune diseases*, vol. 2012, 2012.
- [201] J. A. McBride and R. Striker, “Imbalance in the game of t cells: What can the cd4/cd8 t-cell ratio tell us about hiv and health?” *PLoS pathogens*, vol. 13, no. 11, e1006624, 2017.
- [202] A. Yazdani, M. Raissi, and G. E. Karniadakis, “Systems biology informed deep learning for inferring parameters and hidden dynamics,” *URL <https://www.biorxiv.org/content/early/2019/12/04/865063>*, 2019.
- [203] C. H. Miller, S. G. Maher, and H. A. Young, “Clinical use of interferon- $\gamma$ ,” *Annals of the New York Academy of Sciences*, vol. 1182, p. 69, 2009.
- [204] T. M. Inc., *Ode15s*, Natick, Massachusetts, United States, 2024. [Online]. Available: <https://www.mathworks.com/help/matlab/ref/ode15s.html>.